

Ground-state hyperfine structure of light muon-electron ions

R. N. Faustov,^{1,*} V. I. Korobov^{2,†} A. P. Martynenko^{3,‡} and F. A. Martynenko^{3,§}

¹*Institute of Cybernetics and Informatics in Education, FRC CSC RAS, 119333, Moscow, Russia*

²*Bogoliubov Laboratory of Theoretical Physics JINR, 141980, Dubna, Russia*

³*Samara National Research University, Physics Department, 443086, Samara, Russia*



(Received 13 March 2022; accepted 13 April 2022; published 26 April 2022)

The ground-state hyperfine splitting of light muon-electron ions of lithium, beryllium, boron, and helium is calculated on the basis of analytical perturbation theory in terms of small parameters of the fine-structure constant and electron-muon mass ratio. The corrections of vacuum polarization, nuclear structure, and recoil effects and electron vertex corrections are taken into account. The dependence of the corrections on the nucleus charge Z is studied. The obtained total values of hyperfine splitting intervals can be used for comparison with future experimental data.

DOI: [10.1103/PhysRevA.105.042816](https://doi.org/10.1103/PhysRevA.105.042816)

I. INTRODUCTION

The precision investigation of fine and hyperfine structures of the simplest atoms, gyromagnetic factors of bound leptons, as well as the particle bound states production and decay processes makes it possible to test quantum electrodynamics (QED) and the relativistic theory of bound states. The precision of muonic physics has become especially actualized since 2010, when the first experimental results of low-lying energy level measurements in muonic hydrogen were obtained by the CREMA (charge radius experiments with muonic atoms) collaboration. A decade of active work of this collaboration has brought interesting and unexpected results, related primarily to determining more accurate values of the charge radii of light nuclei (proton, deuteron, helion, alpha particle) [1–5]:

$$\begin{aligned} r_p &= 0.84\,087(26)_{\text{exp}}(29)_{\text{theor}} \text{ fm}, \\ r_d &= 2.12\,718(13)_{\text{exp}}(89)_{\text{theor}} \text{ fm}, \\ r_\alpha &= 1.67\,824(13)_{\text{exp}}(82)_{\text{theor}} \text{ fm}. \end{aligned} \quad (1)$$

As a result of the first experiments of the CREMA collaboration in 2010, the value of proton charge radius $r_p = 0.84\,184(67)$ fm was obtained. It was 10 times more accurate than all previous values from experiments based on electronic systems. Moreover, it was essentially smaller than the CODATA recommended value $r_p = 0.8768(69)$ fm [6]. The difference between these values was named the “proton radius puzzle.” The measurements of energy levels with muonic hydrogen have shown that there is significant discrepancy in the values of proton and deuteron charge radii, emerging from experiments with electronic and muonic atoms. New

problems of studying the fine and hyperfine structures of the energy spectrum are related to muonic ions of lithium, beryllium, etc. [7].

The CREMA experiments caused a series of new experimental studies of that problem. During 2017–2019, different experimental results were obtained, both with electron and muon systems, which made it possible to refine the value of the proton charge radius. The transition frequency ($2S - 4P$) in electronic hydrogen was measured in Ref. [8]: $\Delta\nu_{2S-4P} = 616\,520\,931\,626.8(2.3)$ kHz, and the extracted value of the proton charge radius $r_p = 0.8335(95)$ fm was found to be in agreement with the CREMA result. Another experimental investigation of the proton radius puzzle, PRad (E12-11-1062), was planned in 2011 and successfully carried out in 2016 at the Thomas Jefferson National Accelerator Facility. The PRad experiment was based on the study of electron beams with energy 1.1 and 2.2 GeV. In that experiment, the cross section of the electron-photon (e-p) elastic scattering at unprecedentedly low values of the square of the transferred momentum was measured up to a percentage. The obtained value of the proton charge radius was $r_p = 0.831 \pm 0.007(\text{stat}) \pm 0.012(\text{syst})$ fm [9]. It is less than the average of r_p from previous elastic e-p scattering experiments, but agrees with the spectroscopic results for the muonic hydrogen atom within experimental uncertainties. A new measurement of the electronic hydrogen Lamb shift ($n = 2$) was made in Ref. [10]. The result is $\Delta E^{Ls} = 909.8717(32)$ MHz. The value of the proton charge radius from this experiment, $r_p = 0.833(10)$, agrees with the spectroscopic data for muonic atoms. It should be noted that in another experiment [11], a new measurement of the two-photon transition frequency ($1S - 3S$) was measured with relative uncertainty 9×10^{-13} : $\Delta\nu_{1S-3S} = 2\,922\,743\,278\,671.0(4.9)$ kHz. The value of the proton charge radius from this experiment, $r_p = 0.877(13)$ fm, is in good agreement with the recommended CODATA value. To solve the proton charge radius problem, the PSI MUSE collaboration is planning an experiment to simultaneously measure

*faustov@ccas.ru

†korobov@theor.jinr.ru

‡a.p.martynenko@samsu.ru

§f.a.martynenko@gmail.com

the cross sections for electron and muon scattering by protons [12]. This experiment will make it possible to determine the charge radii of the proton independently in the two reactions and test the lepton universality with an accuracy of an order of magnitude better than previous scattering experiments. At the J-PARC [Muon Science Facility (MUSE)] research center, the MuSEUM collaboration (Japan) plans an order of magnitude more accurate measurement of the hyperfine structure of the muonium ground state [13]. Another experiment of the MU-MASS at PSI (Switzerland) aims to measure the $(1S - 2S)$ transition frequency in muonium with an accuracy of 10 kHz (4 ppt) [14]. New plans for precision microwave spectroscopy of the J-PARC MUSE collaboration [15] involve measuring the hyperfine structure (HFS) of the ground state of muonic helium with an accuracy that is two orders of magnitude better than the previous experiments of the 1980s. The FAMU (Fisica degli Atomi Muonici) collaboration plans to measure the hyperfine structure of the ground state of muonic hydrogen with an accuracy of several ppm [16], and the CREMA [17] collaboration with an accuracy of 1 ppm, using pulsed laser spectroscopy methods. A fundamental experiment related to muon physics is the Fermilab (USA) experiment to measure the muon anomalous magnetic moment [18], which recently confirmed that there is a difference of 4.2 standard deviations between the experimental and theoretical values of the muon anomalous magnetic moment, which can be an indication of the New Physics beyond the Standard Model. Another project with the same goal, but delivered according to a completely different methodology, is planned to be carried out at J-PARC (Japan) [19]. All these experiments, already carried out and planned for the near future, convincingly show that muonic physics, the physics of two-particle and three-particle muonic systems, is currently an urgent problem that requires appropriate theoretical studies and calculations of observable quantities with high accuracy.

In the theoretical study of the energy levels of three-particle electron-muon-nucleus systems, two methods are usually used. One of them is the variational method, which allows one to find wave functions and energies with very high accuracy [20–28] (see other references in the review paper [27]). Basically, theoretical studies were focused on muon-electron helium since measurements of the hyperfine structure of the ground state were performed for it [29,30],

$$\begin{aligned}\Delta\nu_{\text{exp}}^{\text{hfs}}(\mu e_2^3\text{He}) &= 4166.3(2) \text{ MHz}, \\ \Delta\nu_{\text{exp}}^{\text{hfs}}(\mu e_2^4\text{He}) &= 4465.004(29) \text{ MHz}.\end{aligned}\quad (2)$$

An analytical approach for calculating the energy levels of such three-particle systems was formulated in Refs. [31,32] and applied to calculate the hyperfine structure of the spectrum and the electronic Lamb shift in Refs. [33–38]. It is based on the use of the perturbation theory (PT) method with respect to two small parameters: the fine-structure constant α and the electron-muon mass ratio. This approach has certain advantages like any other analytical method. They consist in the fact that the contributions to a certain energy interval are obtained in the form of analytical expressions, which allows better control over the accuracy of the calculations and use

of them for different bound states. In order to achieve high calculation accuracy, it is necessary to calculate numerous corrections in higher orders of perturbation theory.

In our previous paper [38], we calculated the electron Lamb shift $(2P - 2S)$ and the energy interval $(2S - 1S)$ using the analytical method in muon-electron ions of lithium, beryllium, and boron. We showed that the total value of the electronic Lamb shift strongly depends on the charge of the nucleus, so that in the transition from the lithium nucleus to the boron nucleus the magnitude of the shift undergoes a sharp decrease in the case of the beryllium nucleus. In this paper, we continue to study [38] the energy levels of muon-electron ions of lithium, beryllium, and boron in the hyperfine part of the energy spectrum.

II. METHOD FOR CALCULATING BASIC CONTRIBUTIONS TO HFS

The Coulomb interaction in three-particle muon-electronic ions of lithium, beryllium, and boron leads to the formation of bound states. The main features of such three-particle systems are as follows:

(1) The lifetime of such systems is determined by the muon lifetime $\tau_\mu = 2.1969811(22) \times 10^{-6}$ s. From the classical point of view, during this time, the muon manages to make about 10^{13} rotations around the nucleus.

(2) The particle masses satisfy the inequality $m_e \ll m_\mu \ll M$, where m_e is the electron mass, m_μ is the muon mass, and M is the nucleus mass. This leads to the fact that the muon is about 200 times closer to the nucleus than an electron. We can assume that the electron moves in the field of the quasinucleus, which is formed by the muon and the nucleus.

(3) The hyperfine structure of the energy spectrum in the ground state arises from the interaction of particle spins: \mathbf{s}_e is the electron spin, \mathbf{s}_μ is the muon spin, and \mathbf{I} is the nucleus spin. We consider the following as nuclei of lithium, beryllium, and boron isotopes with nuclear spin $I = 3/2$: ${}^7_3\text{Li}$, ${}^9_4\text{Be}$, and ${}^{11}_5\text{B}$. Based on the obtained analytical expressions for various corrections in the hyperfine structure, we also obtained a new splitting estimate for $(\mu e_2^3\text{He})$, $(\mu e_2^4\text{He})$.

To calculate the energy levels by the analytical perturbation theory method, we divide the Hamiltonian of the system into several parts, separating the main contribution of the Coulomb interaction H_0 in the form

$$H = H_0 + \Delta H + \Delta H_{\text{rec}} + \Delta H_{\text{vp}} + \Delta H_{\text{str}} + \Delta H_{\text{vert}},$$

$$H_0 = -\frac{1}{2M_\mu} \nabla_\mu^2 - \frac{1}{2M_e} \nabla_e^2 - \frac{Z\alpha}{x_\mu} - \frac{(Z-1)\alpha}{x_e}, \quad (3)$$

$$\Delta H = \frac{\alpha}{|\mathbf{x}_\mu - \mathbf{x}_e|} - \frac{\alpha}{x_e}, \quad \Delta H_{\text{rec}} = -\frac{1}{M} \nabla_\mu \cdot \nabla_e, \quad (4)$$

where \mathbf{x}_μ and \mathbf{x}_e are the radius vectors of the muon and electron relative to the nucleus, and Ze is the nucleus charge. The terms ΔH_{vp} , ΔH_{str} , and ΔH_{vert} denote contributions of vacuum polarization effects, effects of nucleus structure, and vertex corrections. The reduced masses in the muon-nucleus and electron-nucleus subsystems are equal to

$$M_e = \frac{m_e M}{(m_e + M)}, \quad M_\mu = \frac{m_\mu M}{(m_\mu + M)}. \quad (5)$$

In the initial approximation, which is determined by the Hamiltonian H_0 , the wave function of the system has a simple analytical form,

$$\Psi_0(\mathbf{x}_e, \mathbf{x}_\mu) = \psi_{e0}(\mathbf{x}_e)\psi_{\mu 0}(\mathbf{x}_\mu) = \frac{1}{\pi}(W_e W_\mu)^{3/2} e^{-W_\mu x_\mu} e^{-W_e x_e},$$

$$W_\mu = Z\alpha M_\mu, \quad W_e = (Z-1)\alpha M_e, \quad (6)$$

which allows one to accurately calculate the corrections using the perturbation theory. The Hamiltonian of the hyperfine interaction in the case of the ground state can be presented in the form

$$\Delta H^{\text{hfs}} = \tilde{a}(\mathbf{S}_\mu \cdot \mathbf{I}) - \tilde{b}(\mathbf{S}_e \cdot \mathbf{S}_\mu) + \tilde{c}(\mathbf{S}_e \cdot \mathbf{I}), \quad (7)$$

where the coefficient functions \tilde{a} , \tilde{b} , and \tilde{c} are presented in the form of the expansion by the perturbation theory. In leading order, these functions have the form

$$\tilde{a}_0 = \frac{2\pi\alpha}{3} \frac{g_N g_\mu}{m_p m_\mu} \delta(\mathbf{x}_\mu), \quad \tilde{b}_0 = \frac{2\pi\alpha}{3} \frac{g_\mu g_e}{m_\mu m_e} \delta(\mathbf{x}_\mu - \mathbf{x}_e),$$

$$\tilde{c}_0 = \frac{2\pi\alpha}{3} \frac{g_e g_N}{m_e m_p} \delta(\mathbf{x}_e), \quad (8)$$

where $g_e = 2(1 + a_e)$, $g_\mu = 2(1 + a_\mu)$, and $g_N = \frac{\mu_N}{I}$ are gyromagnetic factors of the electron, muon, and nucleus, μ_N is a nucleus magnetic moment, and $a_{e,\mu}$ are anomalous magnetic moments of the electron and muon.

Averaging the Hamiltonian (7) over the wave functions of the ground state, we obtain

$$v = \langle \Delta H_0^{\text{hfs}} \rangle = a \langle \mathbf{I} \cdot \mathbf{S}_\mu \rangle - b \langle \mathbf{S}_\mu \cdot \mathbf{S}_e \rangle + c \langle \mathbf{S}_e \cdot \mathbf{I} \rangle, \quad (9)$$

where the coefficients

$$a = \sum_{i=0}^{\infty} a_i, \quad b = \sum_{i=0}^{\infty} b_i, \quad c = \sum_{i=0}^{\infty} c_i \quad (10)$$

are determined by different matrix elements by the perturbation theory. Using (6), in leading order, we obtain the following contributions to a , b , c (below, the values for lithium, beryllium, and boron nuclei are given line by line, and for helium nuclei, see Table I):

$$a_0 = \frac{g_N g_\mu}{4} \frac{m_e}{m_p} \left(\frac{W_\mu}{W_e} \right)^3 v_F = \begin{cases} 6.08349 \times 10^8 \text{ MHz}, \\ -5.26948 \times 10^8 \text{ MHz}, \\ 23.66123 \times 10^8 \text{ MHz}. \end{cases}$$

$$v_F = \frac{8\alpha W_e^3}{3m_e m_\mu}, \quad (11)$$

$$b_0 = v_F \frac{g_e g_\mu}{4} \frac{1}{\left(1 + \frac{W_e}{W_\mu}\right)^3} = \begin{cases} 35830.5299 \text{ MHz} \\ 120791.0324 \text{ MHz} \\ 286127.0374 \text{ MHz}, \end{cases} \quad (12)$$

$$c_0 = v_F \frac{m_\mu}{m_p} \frac{g_e g_N}{4} = \begin{cases} 4422.8997 \text{ MHz} \\ -5397.5666 \text{ MHz} \\ 29216.4109 \text{ MHz}. \end{cases} \quad (13)$$

For the calculation of matrix elements from the product of spin operators, we use the following transformation of basis

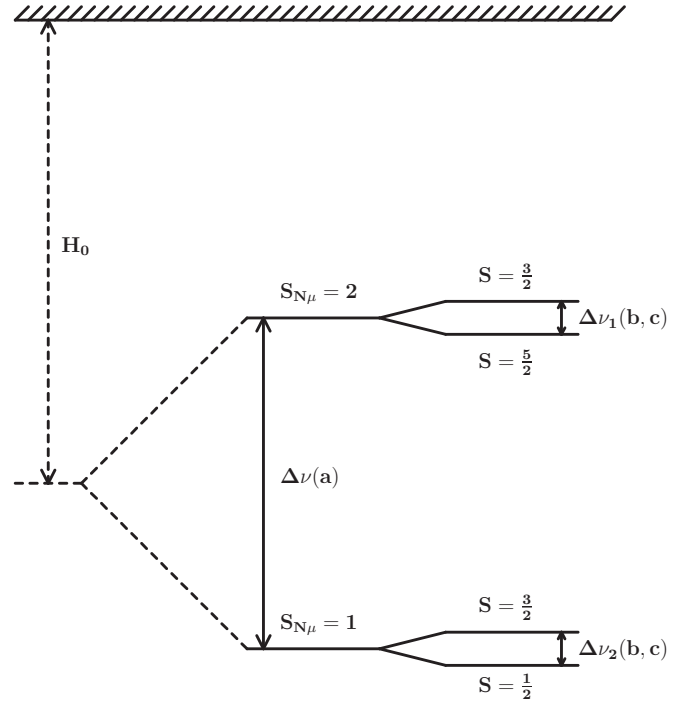


FIG. 1. Hyperfine splitting of the ground state of muon-electron ions of lithium, beryllium, and boron.

wave functions [39]:

$$\Psi_{S_{N\mu} S S_z} = \sum_{S_{Ne}} (-1)^{S_\mu + I + S_e + S} \sqrt{(2S_{N\mu} + 1)(2S_{Ne} + 1)} \times \begin{Bmatrix} S_e & S_N & S_{Ne} \\ S_\mu & S & S_{N\mu} \end{Bmatrix} \Psi_{S_{Ne} S S_z}, \quad (14)$$

where $S_{N\mu}$ is the spin of the muon-nucleus subsystem, S_{Ne} is the spin of the electron-nucleus subsystem, and S is the total spin of the three-particle system. The properties of $6j$ symbols are discussed in [39].

The given numerical values of the main contributions to the coefficients a , b , and c show that the system has small intervals of the hyperfine structure, which are determined by the quantities b and c . An approximate scheme of energy level splitting due to the hyperfine interaction of the ground state is shown in Fig. 1. The coefficient b_0 was calculated using the g factor of the electron, $g_e \approx 2$. The correction connected with the anomalous magnetic moment of an electron in this interaction is considered in Sec. V. When calculating other coefficients, the following values of the gyromagnetic factors are used: $g_e = 2(1 + \kappa_e) = 2[1 + 1.15965218111(74) \times 10^{-3}]$, $g_\mu = 2(1 + \kappa_\mu) = 2[1 + 1.16592069(60) \times 10^{-3}]$, $g_N(^7\text{Li}) = 2.170951$, $g_N(^9\text{Be}) = -0.784955$, $g_N(^{11}\text{B}) = 1.792433$ [40].

The average value of the Hamiltonian of hyperfine interaction ΔH_0^{hfs} calculated in the $\psi_{S_{N\mu} S S_z}$ basis has the form

TABLE I. Contributions to the coefficients b and c in the hyperfine splitting of the ground state in lithium, beryllium, and boron ions, and helium atoms. Table rows in order correspond to $(\mu e^7\text{Li})^+$, $(\mu e^9\text{Be})^{2+}$, $(\mu e^{11}\text{B})^{3+}$, $(\mu e^3\text{He})$, $(\mu e^4\text{He})$.

Contribution to the coefficients b and c	b (MHz)	c (MHz)	Formula
Leading-order contribution of the order of α^4	35830.53 120791.04 286127.05 4487.7131 4488.6167	4422.90 −5397.57 29216.41 −1083.3208 0	(12),(13)
Recoil correction of the order of $\alpha^4 \frac{W_e}{W_\mu}$, $\alpha^4 \frac{W_e^2}{W_\mu^2}$	−155.58 −390.95 −738.06 −29.9789 −29.7371	22.27 −20.36 88.11 −8.3125 0	(32), (35), (A7)
One-loop VP correction in 1γ interaction	0.70 3.99 13.59 0.0357 0.0359	0.17 −0.32 2.29 0.0272 0	(42),(43)
One-loop VP correction in μN interaction in second order of PT	0.69 3.15 9.01 0.0485 0.0484	0 0 0 0 0	(49)
One-loop VP correction in μe interaction in second order of PT	−0.86 −3.07 −7.73 −0.1010 −0.1012	−0.05 0.07 −0.39 0.0090 0	(52),(56), (59),(61)
One-loop VP correction in eN interaction in second order of PT	1.14 5.85 19.00 0.0752 0.0756	0.27 −0.45 3.09 −0.0440 0	(48),(60)
One-loop VP correction with ΔH potential in second order of PT	−0.50 −1.52 −3.28 −0.0704 −0.0732	0.04 −0.05 0.23 −0.0129 0	(65), (69), (71)
Nuclear structure correction in 1γ interaction	0 0 0 0 0	−0.71 1.33 −9.19 0.0696 0	(73)
Nuclear structure correction in 2γ interaction	0 0 0 0 0	−0.49 0.82 −5.27 0.0638 0	(74)
Nuclear structure correction in second order of PT	−0.47 −3.30 −11.77 −0.0132 −0.0097	−0.35 0.44 −2.30 0.0690 0	(76), (77), (78), (79)
Nuclear recoil correction from ΔH_{rec}	0.53 1.38 2.68	0 0 0	(87), (88), (89)

TABLE I. Continued

Contribution to the coefficients b and c	b (MHz)	c (MHz)	Formula
	0.1078	0	
	0.0809	0	
Electron vertex correction of the order of α^5 in 1γ interaction	40.96	0	(91)
	136.73	0	
	320.59	0	
	5.1765	0	
	5.1774	0	
Electron vertex correction of the order of α^5 in second order of PT	-0.06	0	(96),(97),(94)
	-0.06	0	
	0.02	0	
	-0.0209	0	
	-0.0206	0	
Recoil correction in 2γ interaction	6.43	-0.09	(81),(82)
	21.68	0.12	
	51.35	-0.67	
	0.8055	0.0315	
	0.8056	0	
Relativistic correction of the order of α^6	5.77	1.41	(98)
	53.05	-3.88	
	241.24	37.30	
	0.0401	-0.0864	
	0.0401	0	
Radiative correction of the order of α^6	-3.48	-0.64	(99)
	-11.74	1.04	
	-27.82	-7.02	
	-0.4345	0.1041	
	-0.4346	0	
Summary values	35725.80	4444.73	
	120606.23	-5418.81	
	285995.87	29322.59	
	4463.3835	-1091.4024	
	4464.5042	0	

$$\nu = \begin{pmatrix} \Psi_{1, \frac{1}{2}, S_z} & \Psi_{1, \frac{3}{2}, S_z} & \Psi_{2, \frac{3}{2}, S_z} & \Psi_{2, \frac{5}{2}, S_z} \\ \Psi_{1, \frac{1}{2}, S_z} & -\frac{5}{4}a - \frac{1}{4}b - \frac{5}{4}c & 0 & 0 \\ \Psi_{1, \frac{3}{2}, S_z} & 0 & -\frac{5}{4}a + \frac{1}{8}b + \frac{5}{8}c & -\frac{\sqrt{15}}{8}b + \frac{\sqrt{15}}{8}c \\ \Psi_{2, \frac{3}{2}, S_z} & 0 & -\frac{\sqrt{15}}{8}b + \frac{\sqrt{15}}{8}c & \frac{3}{4}a + \frac{3}{8}b - \frac{9}{8}c \\ \Psi_{2, \frac{5}{2}, S_z} & 0 & 0 & 0 \end{pmatrix} \begin{pmatrix} \frac{3}{4}a - \frac{1}{4}b + \frac{3}{4}c \\ 0 \\ 0 \\ 0 \\ 0 \end{pmatrix}. \quad (15)$$

After diagonalizing this matrix, we get four eigenvalues that define the hyperfine structure,

$$\begin{aligned} \nu_1(S_{N\mu} = \tfrac{1}{2}, S = 1) &= -\tfrac{5}{4}a - \tfrac{1}{4}b - \tfrac{5}{4}c, \\ \nu_2(S_{N\mu} = \tfrac{3}{2}, S = 1) &= \tfrac{1}{4}(-a + b - c - \sqrt{16a^2 + 4b^2 + 16c^2 + 4ab - 28ac - 11bc}), \\ \nu_3(S_{N\mu} = \tfrac{3}{2}, S = 2) &= \tfrac{1}{4}(-a + b - c + \sqrt{16a^2 + 4b^2 + 16c^2 + 4ab - 28ac - 11bc}), \\ \nu_4(S_{N\mu} = \tfrac{5}{2}, S = 2) &= \tfrac{3}{4}a - \tfrac{1}{4}b + \tfrac{3}{4}c. \end{aligned} \quad (16)$$

As long as $a \gg b$ and $a \gg c$, we can use expansions in b/a , c/a and represent small intervals of the hyperfine structure in the form

$$\Delta\nu_1^{\text{hfs}} = \nu_3 - \nu_4 = \frac{5(b-3c)}{8} + O\left(\frac{b}{a}, \frac{c}{a}\right), \quad \Delta\nu_2^{\text{hfs}} = \nu_2 - \nu_1 = \frac{3(b+5c)}{8} + O\left(\frac{b}{a}, \frac{c}{a}\right). \quad (17)$$

As it follows from (12), b_0 contains the recoil effects over W_e/W_μ in the leading order in α . The same recoil effects also occur in the second-order perturbation theory in ΔH .

III. RECOIL CORRECTIONS IN SECOND ORDER OF PERTURBATION THEORY

Recoil corrections of the order of $\alpha^4 \frac{W_e}{W_\mu}$, $\alpha^4 \frac{W_e^2}{W_\mu^2} \ln \frac{W_e}{W_\mu}$, and $\alpha^4 \frac{W_e^2}{W_\mu^2}$ occur in the second order of perturbation theory. The contribution to the b coefficient is determined by the following expression:

$$b_1 = 2 \int \Psi^*(\mathbf{x}_e, \mathbf{x}_\mu) \tilde{b}_0(\mathbf{x}_e - \mathbf{x}_\mu) \tilde{G}(\mathbf{x}_e, \mathbf{x}_\mu; \mathbf{x}'_e, \mathbf{x}'_\mu) \Delta H(\mathbf{x}'_e, \mathbf{x}'_\mu) \Psi(\mathbf{x}'_e, \mathbf{x}'_\mu) d\mathbf{x}_e d\mathbf{x}_\mu d\mathbf{x}'_e d\mathbf{x}'_\mu, \quad (18)$$

where the reduced Coulomb Green's function has the form

$$\tilde{G}(\mathbf{x}_e, \mathbf{x}_\mu; \mathbf{x}'_e, \mathbf{x}'_\mu) = \sum_{n, n' \neq 0} \frac{\psi_{\mu n}(\mathbf{x}_\mu) \psi_{en'}(\mathbf{x}_e) \psi_{\mu n}^*(\mathbf{x}'_\mu) \psi_{en'}^*(\mathbf{x}'_e)}{E_{\mu 0} + E_{e0} - E_{\mu n} - E_{en'}}. \quad (19)$$

It is convenient to divide the sum over muon states in (19) into two parts with $n = 0$ and $n \neq 0$. For the first part, we get

$$b_1(n=0) = \frac{4\pi\alpha}{3} \frac{g_e g_\mu}{m_e m_\mu} \int |\psi_{\mu 0}(\mathbf{x}_3)|^2 \psi_{e0}^*(\mathbf{x}_3) \sum_{n' \neq 0} \frac{\psi_{en'}(\mathbf{x}_3) \psi_{en'}^*(\mathbf{x}_1)}{E_{e0} - E_{en'}} V_\mu(\mathbf{x}_1) \psi_{e0}(\mathbf{x}_1) d\mathbf{x}_1 d\mathbf{x}_3, \quad (20)$$

$$V_\mu(\mathbf{x}_1) = \int \psi_{\mu 0}^*(\mathbf{x}_2) \left[\frac{\alpha}{|\mathbf{x}_2 - \mathbf{x}_1|} - \frac{\alpha}{x_1} \right] \psi_{\mu 0}(\mathbf{x}_2) d\mathbf{x}_2 = -\frac{\alpha}{x_1} (1 + W_\mu x_1) e^{-2W_\mu x_1}. \quad (21)$$

The reduced Coulomb Green's function of an electron in (20) is determined by [41]

$$G_e(\mathbf{x}_1, \mathbf{x}_3) = \sum_{n \neq 0} \frac{\psi_{en}(\mathbf{x}_3) \psi_{en}^*(\mathbf{x}_1)}{E_{e0} - E_{en}} = -\frac{W_e M_e}{\pi} e^{-W_e(x_1 + x_3)} \left[\frac{1}{2W_e x_>} - \ln(2W_e x_>) - \ln(2W_e x_<) + \text{Ei}(2W_e x_<) \right. \\ \left. + \frac{7}{2} - 2C - W_e(x_1 + x_3) + \frac{1 - e^{2W_e x_<}}{2W_e x_<} \right], \quad (22)$$

where $x_< = \min(x_1, x_3)$, $x_> = \max(x_1, x_3)$, $C = 0.577216 \dots$ is the Euler constant and $\text{Ei}(x)$ is the integral exponential function. Then the coordinate integration in (20) can be performed analytically, and the obtained result can be represented as an expansion in W_e/W_μ ,

$$b_1(n=0) = \nu_F \frac{(1 + \kappa_\mu)}{(Z-1)} \left[\frac{11}{8} \frac{W_e}{W_\mu} - \frac{1}{16} \frac{W_e^2}{W_\mu^2} \left(64 \ln \frac{W_e}{W_\mu} + 64 \ln 2 + 7 \right) \right]. \quad (23)$$

Excited states of the muon ($n \neq 0$) give the second part of the contribution to the b coefficient,

$$b_1(n \neq 0) = \frac{4\pi\alpha}{3} \frac{g_e g_\mu}{m_e m_\mu} \int \psi_{\mu 0}^*(\mathbf{x}_3) \psi_{e0}^*(\mathbf{x}_3) \sum_{n \neq 0} \psi_{\mu n}(\mathbf{x}_3) \psi_{\mu n}^*(\mathbf{x}_2) G_e(\mathbf{x}_3, \mathbf{x}_1, z) \times \left[\frac{\alpha}{|\mathbf{x}_2 - \mathbf{x}_1|} - \frac{\alpha}{x_1} \right] \psi_{\mu 0}(\mathbf{x}_2) \psi_{e0}(\mathbf{x}_1) d\mathbf{x}_1 d\mathbf{x}_2 d\mathbf{x}_3, \quad (24)$$

where we introduce the electron Green's function,

$$G_e(\mathbf{x}_3, \mathbf{x}_1, z) = \sum_{n' \neq 0} \frac{\psi_{en'}(\mathbf{x}_3) \psi_{en'}^*(\mathbf{x}_1)}{z - E_{en'}} = \sum_{n' \neq 0} \frac{\psi_{en'}(\mathbf{x}_3) \psi_{en'}^*(\mathbf{x}_1)}{E_{\mu 0} + E_{e0} - E_{\mu n} - E_{en'}}. \quad (25)$$

The term $(-\alpha/x_1)$ in (24) does not contribute due to the orthogonality of the muon wave functions. To perform further analytic integration in (22), we replace G_e approximately with the free Green's function [31,32],

$$G_e(\mathbf{x}_3, \mathbf{x}_1, E_{\mu 0} + E_{e0} - E_{\mu n}) \rightarrow G_{e0}(\mathbf{x}_3 - \mathbf{x}_1, E_{\mu 0} + E_{e0} - E_{\mu n}) = -\frac{M_e}{2\pi} \frac{e^{-\beta|\mathbf{x}_3 - \mathbf{x}_1|}}{|\mathbf{x}_3 - \mathbf{x}_1|}, \quad (26)$$

where $\beta = \sqrt{2M_e(E_{\mu n} - E_{e0} - E_{\mu 0})}$. In addition, we approximately replace wave functions of an electron in (22) by their values at zero, $\psi_{e0}(0)$. The terms omitted in this approximation can give a second-order contribution with respect to $\frac{W_e}{W_\mu}$ in b . The results of numerical integration in [31] with the exact Green's function of the electron in the case of muonic helium show that the terms used in the (26) approximation are numerically small.

After these approximations, the integration over the \mathbf{x}_1 coordinate gives the following result:

$$\int \frac{e^{-\beta|\mathbf{x}_3 - \mathbf{x}_1|}}{|\mathbf{x}_3 - \mathbf{x}_1|} \frac{d\mathbf{x}_1}{|\mathbf{x}_2 - \mathbf{x}_1|} = 4\pi \left[\frac{1}{\beta} - \frac{1}{2} |\mathbf{x}_3 - \mathbf{x}_2| + \frac{1}{6} \beta |\mathbf{x}_3 - \mathbf{x}_2|^2 - \frac{\beta^2}{24} |\mathbf{x}_3 - \mathbf{x}_2|^3 + \dots \right], \quad (27)$$

where an expansion of $e^{-\beta|\mathbf{x}_2 - \mathbf{x}_3|}$ in $\beta|\mathbf{x}_2 - \mathbf{x}_3|$ is done. This expansion is equivalent to the expansion in powers of $\sqrt{W_e/W_\mu}$. The first expansion term β^{-1} in (27) does not contribute to (24). The second expansion term in (27) gives the leading-order

contribution in $\sqrt{W_e/W_\mu}$: $-\nu_F \frac{35W_e}{8(Z-1)W_\mu}$. To increase the accuracy of the result, we also consider the third term on the right side (27), which leads to the following integral:

$$\int \psi_{\mu 0}^*(\mathbf{x}_3) \sum_n \sqrt{2M_e(E_{\mu n} - E_{\mu 0})} \psi_{\mu n}(\mathbf{x}_3) \psi_{\mu n}^*(\mathbf{x}_2) (\mathbf{x}_2 \cdot \mathbf{x}_3) \psi_{\mu 0}(\mathbf{x}_2) d\mathbf{x}_2 d\mathbf{x}_3 = \sqrt{\frac{W_e Z}{W_\mu^3(Z-1)}} S_{\frac{1}{2}}, \quad (28)$$

where we introduce the quantity

$$S_{1/2} = \sum_n \left(\frac{E_{\mu n} - E_{\mu 0}}{R_\mu} \right)^{1/2} |\langle \mu 0 | \frac{\mathbf{x}}{a_\mu} | \mu n \rangle|^2, \quad R_\mu = \frac{1}{2} M_\mu (Z\alpha)^2. \quad (29)$$

A contribution to (29) comes from matrix elements for discrete and continuous states, which are presented in [42]. The numerical contributions of discrete and continuous states to (29) have the form

$$S_{\frac{1}{2}}^d = \sum_n \frac{2^8 n^6 (n-1)^{2n-\frac{9}{2}}}{(n+1)^{2n+\frac{9}{2}}} = 1.90\,695\dots, \quad (30)$$

$$S_{\frac{1}{2}}^c = \int_0^\infty \frac{2^8 k dk}{(k^2 + 1)^{9/2} (1 - e^{-\frac{2\pi}{k}})} \left| \left(\frac{1 + ik}{1 - ik} \right)^{i/k} \right| = 1.03\,111\dots \quad (31)$$

Adding the recoil corrections (23) and (24) in the second order of perturbation theory, we get the total recoil correction to b of the order of α^4 as follows:

$$b_1 = \nu_F \frac{(1 + \kappa_\mu)}{(Z-1)} \left[-3 \frac{W_e}{W_\mu} + \frac{231W_e^2}{32W_\mu^2} - \frac{4W_e^2}{W_\mu^2} \ln \frac{2W_e}{W_\mu} + \frac{4W_e}{3W_\mu} \sqrt{\frac{W_e Z}{W_\mu(Z-1)}} S_{1/2} \right]. \quad (32)$$

In the second order of perturbation theory, we have a similar contribution to the coefficient c . To calculate it, it is necessary to choose the hyperfine part of the perturbation operator in the form $\Delta H_0^{\text{hfs}}(\mathbf{x}_e) = \frac{2\pi\alpha}{3} \frac{g_e g_N}{m_e m_p} \delta(\mathbf{x}_e)$ in a general expression like (24). Using then the obvious simplifications connected with the δ function, one can transform the recoil correction to c as follows:

$$c_1 = \frac{4\pi\alpha}{3} \frac{g_e g_N}{m_e m_p} \int \psi_{e0}^*(0) \tilde{G}_e(0, \mathbf{x}_1) V_\mu(\mathbf{x}_1) \psi_{e0}(\mathbf{x}_1) d\mathbf{x}_1. \quad (33)$$

The reduced Coulomb Green's function of an electron with one zero argument in this equation is equal to

$$\tilde{G}_e(0, \mathbf{x}) = \sum_{n \neq 0} \frac{\psi_{en}(0) \psi_{en}^*(\mathbf{x})}{E_{e0} - E_{en}} = -\frac{W_e M_e}{\pi} e^{-W_e x} \left[\frac{1}{2W_e x} - \ln 2W_e x + \frac{5}{2} - C - W_e x \right]. \quad (34)$$

As a result of the analytical calculation of matrix elements over coordinate variables, we get a contribution to the coefficient c . It can be presented in the form of an expansion in W_e/W_μ ,

$$c_1 = c_0 \frac{2}{(Z-1)} \left[\frac{3W_e}{2W_\mu} + 2 \frac{W_e^2}{W_\mu^2} \left(\frac{1}{4} - \ln \frac{W_e}{W_\mu} \right) \right]. \quad (35)$$

Numerical values of contribution (35) for various muon-electron ions are presented in Table I.

IV. EFFECTS OF VACUUM POLARIZATION

Among other corrections in the energy spectrum of muonic atoms and ions, corrections of vacuum polarization [43,44] stand out. The one-loop vacuum polarization, which is taken into account in this paper, gives a fifth-order contribution in α to the HFS. The corresponding interaction amplitudes in the first and second orders of the perturbation theory are shown schematically in Figs. 2 and 3.

The correction for vacuum polarization in the first-order perturbation theory is related to the modification of the hyperfine part of the Hamiltonian (7) [see Fig. 2(a)], which has the following form in the case of muon-electron and electron-nuclear interactions:

$$\Delta V_{\text{vp}, e\mu}^{\text{hfs}}(\mathbf{x}_{e\mu}) = -\frac{2\alpha g_e g_\mu}{3m_e m_\mu} (\mathbf{S}_e \cdot \mathbf{S}_\mu) \frac{\alpha}{3\pi} \int_1^\infty \rho(\xi) d\xi \left[\pi \delta(\mathbf{x}_{e\mu}) - \frac{m_e^2 \xi^2}{x_{e\mu}} e^{-2m_e \xi x_{e\mu}} \right], \quad (36)$$

$$\Delta V_{\text{vp}, eN}^{\text{hfs}}(\mathbf{x}_e) = \frac{2\alpha g_e g_N}{3m_e m_p} (\mathbf{S}_e \cdot \mathbf{I}) \frac{\alpha}{3\pi} \int_1^\infty \rho(\xi) d\xi \left[\pi \delta(\mathbf{x}_e) - \frac{m_e^2 \xi^2}{x_e} e^{-2m_e \xi x_e} \right], \quad (37)$$

$$\rho(\xi) = \frac{\sqrt{\xi^2 - 1} (2\xi^2 + 1)}{\xi^4}. \quad (38)$$

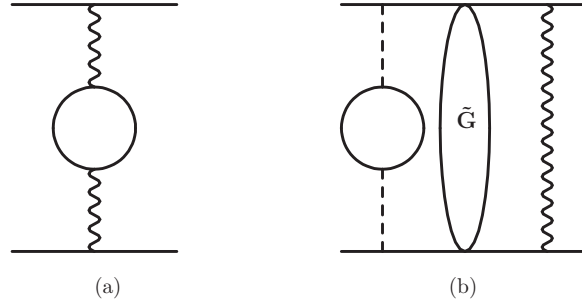


FIG. 2. Correction of vacuum polarization. Dashed line denotes the contribution of the Coulomb photon. The wavy line denotes the hyperfine part of the Breit potential. \tilde{G} denotes the reduced Coulomb Green's function.

The matrix element of the potential (36) with wave functions (6) gives the contribution to coefficient b ,

$$b_{vp} = \frac{8\alpha^2}{9m_em_\mu} \frac{W_e^3 W_\mu^3}{\pi^3} \int_1^\infty \rho(\xi) d\xi \int d\mathbf{x}_e \int d\mathbf{x}_\mu e^{-2W_\mu x_\mu} e^{-2W_e x_e} \times \left[\pi \delta(\mathbf{x}_\mu - \mathbf{x}_e) - \frac{m_e^2 \xi^2}{|\mathbf{x}_\mu - \mathbf{x}_e|} e^{-2m_e \xi |\mathbf{x}_\mu - \mathbf{x}_e|} \right]. \quad (39)$$

Both integrals over coordinates of the muon and electron in (39) can be calculated analytically,

$$I_1 = \int d\mathbf{x}_e \int d\mathbf{x}_\mu e^{-2W_\mu x_\mu} e^{-2W_e x_e} \pi \delta(\mathbf{x}_\mu - \mathbf{x}_e) = \frac{\pi^2}{W_\mu^3 \left(1 + \frac{W_e}{W_\mu}\right)^3}, \quad (40)$$

$$I_2 = \int d\mathbf{x}_e \int d\mathbf{x}_\mu e^{-2W_\mu x_\mu} e^{-2W_e x_e} \frac{m_e^2 \xi^2}{|\mathbf{x}_\mu - \mathbf{x}_e|} e^{-2m_e \xi |\mathbf{x}_\mu - \mathbf{x}_e|} \\ = \frac{\pi^2 m_e^2 \xi^2}{W_\mu^5} \frac{\left[\frac{W_e^2}{W_\mu^2} + \left(1 + \frac{m_e \xi}{W_\mu}\right)^2 + \frac{W_e}{W_\mu} \left(3 + \frac{2m_e \xi}{W_\mu}\right) \right]}{\left(1 + \frac{W_e}{W_\mu}\right)^3 \left(1 + \frac{m_e \xi}{W_\mu}\right)^2 \left(\frac{W_e}{W_\mu} + \frac{m_e \xi}{W_\mu}\right)^2}. \quad (41)$$

Separately integrals over the spectral parameter ξ in (40) and (41) are divergent. But their sum is finite and can be presented as follows:

$$b_{vp} = v_F \frac{\alpha W_e}{3\pi W_\mu \left(1 + \frac{W_e}{W_\mu}\right)^3} \int_1^\infty \rho(\xi) d\xi \frac{\left[\frac{W_e}{W_\mu} + 2 \frac{m_e \xi}{W_\mu} \frac{W_e}{W_\mu} + \frac{m_e \xi}{W_\mu} \left(2 + \frac{m_e \xi}{W_\mu}\right) \right]}{\left(1 + \frac{m_e \xi}{W_\mu}\right)^2 \left(\frac{W_e}{W_\mu} + \frac{m_e \xi}{W_\mu}\right)^2}. \quad (42)$$

The order of contribution (42) is determined by two small parameters α and W_e/W_μ . The correction b_{vp} has the fifth order in α and the first order in W_e/W_μ . The integration over ξ in (42) is done numerically. The result is presented in Table I.

The contribution of the muon vacuum polarization is much smaller than (42) and is not taken into account when obtaining the total numerical value of the hyperfine splitting. We also neglect the contribution of two-loop vacuum polarization, which is suppressed by an additional factor α/π .

The contribution of the correction of one-loop vacuum polarization to the coefficient c has the order α^6 . It can be calculated in the same way using potential (37) ($\alpha_1 = W_e/m_e$). After integration over all variables, including ξ , we obtain

$$c_{vp} = v_F \frac{\alpha g_N m_\mu}{6\pi m_p} \frac{\sqrt{1 - \alpha_1^2} (6\alpha_1 + \alpha_1^3 - 3\pi) + (6 - 3\alpha_1^2 + 6\alpha_1^4) \arccos \alpha_1}{3\alpha_1^3 \sqrt{1 - \alpha_1^2}}. \quad (43)$$

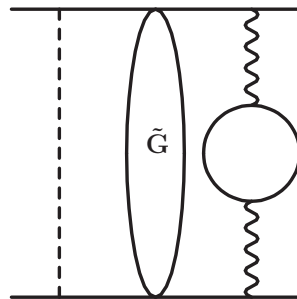


FIG. 3. Effects of vacuum polarization in second order of perturbation theory. Dashed line denotes the potential ΔH (3). The wavy line denotes the hyperfine part of the Breit potential.

When calculating corrections in the second-order perturbation theory, it is necessary to use the following expressions for the Coulomb potentials as one of the perturbation operators, taking into account the vacuum polarization effect [45–47]:

$$\Delta V_{\text{vp}}^{eN}(x_e) = \frac{\alpha}{3\pi} \int_1^\infty \rho(\xi) \left(-\frac{Z\alpha}{x_e}\right) e^{-2m_e \xi x_e} d\xi, \quad (44)$$

$$\Delta V_{\text{vp}}^{\mu N}(x_\mu) = \frac{\alpha}{3\pi} \int_1^\infty \rho(\xi) \left(-\frac{Z\alpha}{x_\mu}\right) e^{-2m_e \xi x_\mu} d\xi, \quad (45)$$

$$\Delta V_{\text{vp}}^{e\mu}(|\mathbf{x}_e - \mathbf{x}_\mu|) = \frac{\alpha}{3\pi} \int_1^\infty \rho(\xi) \frac{\alpha}{x_{e\mu}} e^{-2m_e \xi x_{e\mu}} d\xi, \quad (46)$$

where $x_{e\mu} = |\mathbf{x}_e - \mathbf{x}_\mu|$.

The original integral expression for the contribution to b from the electron-nuclear potential (44) in second-order perturbation theory has the form

$$b_{\text{vp, sopt}}^{eN} = \frac{4\pi\alpha g_e g_\mu}{3m_e m_\mu} \int d\mathbf{x}_1 \int d\mathbf{x}_2 \int d\mathbf{x}_3 \frac{\alpha}{3\pi} \int_1^\infty \rho(\xi) d\xi \psi_{\mu 0}^*(\mathbf{x}_3) \psi_{e 0}^*(\mathbf{x}_3) \\ \times \sum_{n, n' \neq 0} \frac{\psi_{\mu n}(\mathbf{x}_3) \psi_{e n'}(\mathbf{x}_3) \psi_{\mu n}^*(\mathbf{x}_2) \psi_{e n'}^*(\mathbf{x}_1)}{E_{\mu 0} + E_{e 0} - E_{\mu n} - E_{e n'}} \left(-\frac{Z\alpha}{x_1}\right) e^{-2m_e \xi x_1} \psi_{\mu 0}(\mathbf{x}_2) \psi_{e 0}(\mathbf{x}_1), \quad (47)$$

where the subscript “sopt” is used to denote the second-order perturbation theory contribution. The summation in (47) is performed over the entire set of electron and muon states, excluding the state with $n, n' = 0$. Using the orthogonality of muon wave functions, the correction (47) can be represented in integral form,

$$b_{\text{vp, sopt}}^{eN} = v_F \frac{Z\alpha a_2^2}{3(Z-1)\pi} \int_1^\infty \rho(\xi) d\xi \int_0^\infty x_3^2 dx_3 \int_0^\infty x_1 dx_1 e^{-\gamma_1(1+\gamma_3)x_1} e^{-x_3(1+\gamma_1)} \\ \times \left[\frac{1}{\gamma_1 x_3} - \ln(\gamma_1 x_3) - \ln(\gamma_1 x_1) + \text{Ei}(\gamma_1 x_3) + \frac{7}{2} - 2C - \frac{\gamma_1}{2}(x_1 + x_3) \right. \\ \left. + \frac{1 - e^{\gamma_1 x_3}}{\gamma_1 x_3} \right] = v_F \frac{Z\alpha}{3(Z-1)\pi(1+\gamma_1)^4} \int_1^\infty \frac{\rho(\xi) d\xi}{(1+\gamma_3)^3(1+\gamma_3\gamma_1+\gamma_1)^2} \\ \times \left\{ 3 + \gamma_3(7+2\gamma_3) + \gamma_1\{6 + \gamma_3[20 + \gamma_3(13+\gamma_3)]\} + (1+\gamma_3)[3 + 2\gamma_3(5+2\gamma_3)]\gamma_1^2 \right. \\ \left. + 2(1+\gamma_3)(1+\gamma_1)(1+\gamma_1+\gamma_3\gamma_1) \ln \left[1 - \frac{\gamma_3}{(1+\gamma_3)(1+\gamma_1)} \right] \right\}, \quad \gamma_3 = \frac{m_e \xi}{W_e}, \quad \gamma_1 = \frac{W_e}{W_\mu}. \quad (48)$$

The integration over particle coordinates is carried out analytically. The integration over ξ is done numerically. Numerical results are presented in Table I.

A similar calculation can be performed in the case of a potential with muon-nuclear vacuum polarization (45). The electron remains in the $1S$ state, and the reduced Coulomb Green’s function of the system is transformed into the muon Green’s function. In this case, the correction to the coefficient b can be represented as an integral,

$$b_{\text{vp, sopt}}^{\mu N} = v_F \frac{\alpha}{3\pi} \int_1^\infty \frac{\rho(\xi) d\xi}{(\gamma_3+1)^3(\gamma_1+1)^4(\gamma_3+\gamma_1+1)^2} \left[\gamma_1 \{ \gamma_3^3(\gamma_1+4) + \gamma_3^2[\gamma_1(2\gamma_1+13) + 14] \right. \\ \left. + \gamma_3(\gamma_1+1)(7\gamma_1+13) + 3(\gamma_1+1)^2 \} + 2(\gamma_3+1)(\gamma_1+1)(\gamma_3+\gamma_1+1)^2 \ln \frac{(\gamma_3+1)(\gamma_1+1)}{(\gamma_3+\gamma_1+1)} \right]. \quad (49)$$

The second-order perturbation theory correction to b , which is determined by the potential (36), turns out to be the most difficult to calculate. In this case, it is necessary to take into account intermediate excited states for both the electron and the muon. We break this contribution into two parts. The first part, in which the muon is in the $1S$ intermediate state, has the form

$$b_{\text{vp, sopt}}^{\mu e}(n=0) = \frac{256\alpha^2 W_e^3 W_\mu^3}{9\pi m_e m_\mu} \int_0^\infty x_3^2 dx_3 e^{-(W_e+2W_\mu)x_3} \times \int_0^\infty x_1^2 dx_1 e^{-W_e x_1} \int_1^\infty \rho(\xi) d\xi \Delta V_{\text{vp}, \mu}(x_1) G_e(x_1, x_3), \quad (50)$$

where function $V_{\text{vp}, \mu}(x_1)$ is

$$\Delta V_{\text{vp}, \mu}(x_1) = \frac{W_\mu^3}{\pi} \int d\mathbf{x}_2 e^{-2W_\mu x_2} \frac{\alpha}{|\mathbf{x}_1 - \mathbf{x}_2|} e^{-2m_e \xi |\mathbf{x}_1 - \mathbf{x}_2|} \\ = \frac{\alpha W_\mu^3}{x_1(W_\mu^2 - m_e^2 \xi^2)^2} [W_\mu (e^{-2m_e \xi x_1} - e^{-2W_\mu x_1}) + x_1 (m_e^2 \xi^2 - W_\mu^2) e^{-2W_\mu x_1}]. \quad (51)$$

Substituting (51) into (50) and integrating over particle coordinates, we get

$$b_{\text{vp,sopt}}^{\mu e}(n=0) = -v_F \frac{\alpha \gamma_1}{3\pi(Z-1)(1+\gamma_1)^4} \int_1^\infty \frac{\rho(\xi)d\xi}{(1-\gamma_3^2)^2} \left\{ -\frac{6(-1+\gamma_3^2)}{(1+\gamma_1)^3} + \frac{(-6+11\gamma_3^2)}{(1+\gamma_1)^2} \right. \\ - \frac{(1+7\gamma_3^2)}{(1+\gamma_1)} + \frac{(-1+\gamma_3^2)}{(2+\gamma_1)^3} + \frac{(3-4\gamma_3^2)}{(2+\gamma_1)^2} + \frac{(-2+7\gamma_3^2)}{(2+\gamma_1)} + \frac{2(-1+\gamma_3)\gamma_3^2}{(\gamma_3+\gamma_1)^3} - \frac{\gamma_3[-1+\gamma_3(5+\gamma_3)]}{(\gamma_3+\gamma_1)^2} \\ + \frac{3+5\gamma_3^2}{(\gamma_3+\gamma_1)} + \frac{\gamma_3^3}{(1+\gamma_3+\gamma_1)^2} - \frac{5\gamma_3^2}{1+\gamma_3+\gamma_1} + \frac{2\gamma_1(-2+\gamma_3^2-\gamma_1)}{(1+\gamma_1)^2} \ln \frac{1+\gamma_1}{2+\gamma_1} + \frac{2\gamma_1}{(\gamma_3+\gamma_1)^2} \ln \frac{\gamma_3+\gamma_1}{1+\gamma_3+\gamma_1} \\ \left. + \frac{2\gamma_1}{(1+\gamma_1)^2(\gamma_3+\gamma_1)^2} \left[-(-1+\gamma_3)^2(1+\gamma_3^2+2\gamma_3(1+\gamma_1)+\gamma_1(3+\gamma_1)) \ln \frac{\gamma_1}{1+\gamma_1} \right] \right\}. \quad (52)$$

The integration over the parameter ξ is performed numerically. The second part of the correction under consideration to b can initially be represented as

$$b_{\text{vp,sopt}}^{\mu e}(n \neq 0) = -\frac{4\alpha^2}{9\pi} \frac{g_e g_\mu}{m_e m_\mu} \int d\mathbf{x}_3 \int d\mathbf{x}_2 \int_1^\infty \rho(\xi)d\xi \psi_{\mu 0}^*(\mathbf{x}_3) \psi_{e 0}^*(\mathbf{x}_3) \\ \times \sum_{n \neq 0} \psi_{\mu n}(\mathbf{x}_3) \psi_{\mu n}^*(\mathbf{x}_2) \frac{M_e}{2\pi} \frac{e^{-\beta|\mathbf{x}_3-\mathbf{x}_1|}}{|\mathbf{x}_3-\mathbf{x}_1|} \frac{\alpha}{|\mathbf{x}_2-\mathbf{x}_1|} e^{-2m_e \xi |\mathbf{x}_2-\mathbf{x}_1|} \psi_{\mu 0}(\mathbf{x}_2) \psi_{e 0}(\mathbf{x}_1), \quad (53)$$

where, as before, the exact electron Coulomb Green's function is replaced by the free one. Replacing also the electronic wave functions with their values at zero, we thus neglect the same recoil corrections and can perform analytical integration over \mathbf{x}_1 ,

$$J = \int d\mathbf{x}_1 \frac{e^{-\beta|\mathbf{x}_3-\mathbf{x}_1|}}{|\mathbf{x}_3-\mathbf{x}_1|} \frac{e^{-2m_e \xi |\mathbf{x}_2-\mathbf{x}_1|}}{|\mathbf{x}_2-\mathbf{x}_1|} = -\frac{4\pi}{|\mathbf{x}_3-\mathbf{x}_2|} \frac{1}{\beta^2 - 4m_e^2 \xi^2} [e^{-\beta|\mathbf{x}_3-\mathbf{x}_2|} - e^{-2m_e \xi |\mathbf{x}_3-\mathbf{x}_2|}] \\ = 2\pi \left[\frac{(1 - e^{-2m_e \xi |\mathbf{x}_3-\mathbf{x}_2|})}{2m_e^2 \xi^2 |\mathbf{x}_3-\mathbf{x}_2|} - \frac{\beta}{2m_e^2 \xi^2} + \frac{(1 - e^{-2m_e \xi |\mathbf{x}_3-\mathbf{x}_2|})\beta^2}{8m_e^4 \xi^4 |\mathbf{x}_3-\mathbf{x}_2|} + \frac{\beta^2 |\mathbf{x}_3-\mathbf{x}_2|}{4m_e^2 \xi^2} - \frac{\beta^3}{8m_e^4 \xi^4} - \frac{\beta^3 (\mathbf{x}_3-\mathbf{x}_1)^2}{12m_e^2 \xi^2} + \dots \right], \quad (54)$$

where, after an integration, the expansion in $\beta|\mathbf{x}_3-\mathbf{x}_2|$ is used. For further transformations, it is convenient to use the completeness condition,

$$\sum_{n \neq 0} \psi_{\mu n}(\mathbf{x}_3) \psi_{\mu n}^*(\mathbf{x}_2) = \delta(\mathbf{x}_3 - \mathbf{x}_2) - \psi_{\mu 0}(\mathbf{x}_3) \psi_{\mu 0}^*(\mathbf{x}_2). \quad (55)$$

The second and fifth terms in this expansion do not contribute due to the orthogonality of the muon wave functions. The first term in square brackets gives the main contribution with respect to α and W_e/W_μ ($\gamma = m_e \xi / W_\mu$), which can be split into two parts according to (55),

$$b_{\text{vp,sopt}}^{\mu e}(n \neq 0) = b_{\text{vp,1}} + b_{\text{vp,2}}, \quad b_{\text{vp,1}} = -\frac{3\alpha^2 M_e}{8m_e} v_F, \quad (56) \\ b_{\text{vp,2}} = v_F \frac{\alpha^2 M_e}{24\pi m_e} \int_1^\infty \frac{\rho(\xi)d\xi}{\xi} \frac{\{16 + \gamma[5\gamma(\gamma+4) + 29]\}}{(1+\gamma)^4}. \quad (57)$$

The total numerical value $b_{\text{vp,1}} + b_{\text{vp,2}}$ is included in Table I.

Other terms in (53) are calculated as well. With the fourth term in (53), which is proportional to $\beta^2 = 2M_e(E_{\mu n} - E_{\mu 0})$, we can do a number of transformations:

$$\sum_{n=0}^\infty E_{\mu n} \int d\mathbf{x}_2 \int d\mathbf{x}_3 \psi_{\mu 0}^*(\mathbf{x}_2) \psi_{\mu n}(\mathbf{x}_3) \psi_{\mu n}^*(\mathbf{x}_2) |\mathbf{x}_3 - \mathbf{x}_2| \psi_{\mu 0}(\mathbf{x}_2) \\ = \int d\mathbf{x}_2 \int d\mathbf{x}_3 \delta(\mathbf{x}_3 - \mathbf{x}_2) \left[-\frac{\nabla_3^2}{2M_\mu} |\mathbf{x}_3 - \mathbf{x}_2| \psi_{\mu 0}^*(\mathbf{x}_3) \right] \psi_{\mu 0}(\mathbf{x}_2). \quad (58)$$

The expression (58) is divergent due to the δ function. The same divergence take place in another term with β^2 in square brackets in (53). But their sum gives a finite result,

$$b_{\beta^2} = v_F \frac{9\alpha W_e^2}{32m_e W_\mu} \left(1 + \frac{5}{72} \frac{W_\mu^2}{m_e^2} \right). \quad (59)$$

Numerically, this correction is significantly smaller than the leading-order term in (53). Other terms in (53) can be neglected.

The interaction potential (44) does not contain the muon coordinate. The corresponding contribution to the coefficient c in the second-order perturbation theory can be obtained by setting $n=0$ for the muon state in the Coulomb Green's function. Moreover, the presence of $\delta(\mathbf{x}_e)$ in the perturbation operator gives the electron Green's function with one zero argument. As a result, the contribution to c can be represented in integral form,

$$c_{\text{vp,sopt}}^{eN} = v_F \frac{\alpha m_\mu g_e g_N}{4\pi m_p} \int_1^\infty \rho(\xi)d\xi \\ \times \frac{2\gamma_3^2 + 3\gamma_3 + 2\gamma_3 \ln \gamma_3 - 2}{2\gamma_3^3}. \quad (60)$$

The vacuum polarization potential in the Coulomb muon-nuclear ($\mu - N$) interaction does not contribute to c in the second-order perturbation theory due to the orthogonality of the muon wave functions.

Let us consider the calculation of the correction to c from the potential (46) in the second-order perturbation theory. The necessary contribution is determined only by

the intermediate muon state with $n = 0$ in the Green's function. Using (56), this correction can be represented as

$$c_{\text{vp, sopt}}^{e\mu} = -v_F \frac{\alpha m_\mu g_N W_e^2}{6\pi m_p W_\mu^2} \int_1^\infty \frac{\rho(\xi) d\xi}{(1-\gamma^2)^2} \left[\frac{3\gamma^2 \gamma_1^2}{(\gamma_1+1)^4} - \frac{\gamma^2}{(\gamma_1+1)^2} - \frac{2\gamma^2 \gamma_1}{(\gamma_1+1)^3} + \frac{2\gamma_1^2}{(\gamma+\gamma_1)^3} \right. \\ \left. - \frac{2}{(\gamma+\gamma_1)} - \frac{3\gamma_1}{(\gamma+\gamma_1)^2} - \frac{2\gamma_1^2}{(\gamma_1+1)^3} - \frac{3\gamma_1^2}{(\gamma_1+1)^4} + \frac{2}{(\gamma_1+1)} + \frac{3\gamma_1}{(\gamma_1+1)^2} + \frac{2\gamma_1}{(\gamma_1+1)^3} \right. \\ \left. - \frac{2\gamma_1 \ln(\gamma+\gamma_1)}{(\gamma+\gamma_1)^2} + \frac{2\gamma_1(\gamma_1+2-\gamma^2) \ln(\gamma_1+1)}{(\gamma_1+1)^3} + \frac{2(\gamma-1)^2 \gamma_1 [\gamma^2 + 2\gamma(\gamma_1+1) + \gamma_1^2 + 3\gamma_1 + 1] \ln \gamma_1}{(\gamma_1+1)^3 (\gamma+\gamma_1)^2} \right]. \quad (61)$$

There is also a second-order contribution of perturbation theory to the HFS, in which one of the perturbation potentials is determined by (36) and (37) (see Fig. 3), and the second is equal to ΔH . Dividing the correction in the hyperfine structure into two parts, we first calculate the part with $n = 0$ for the muon ground state. The second part with $n \neq 0$ contains excited muon states. In turn, the term with $n = 0$ can also be divided into two parts, and the first part with the δ function in (36) gives the following contribution to b :

$$b_{\text{vp, sopt}}^{(1)}(n=0) = v_F \frac{\alpha}{3\pi} \int_1^\infty \rho(\xi) d\xi \frac{11W_e}{16W_\mu}. \quad (62)$$

The integral over the spectral parameter ξ is divergent, so we must consider the second term in the potential (36), whose contribution to b will be given by

$$b_{\text{vp, sopt}}^{(2)}(n=0) = \frac{16\alpha^2 m_e^2}{9\pi m_e m_\mu} \int_1^\infty \rho(\xi) \xi^2 d\xi \int d\mathbf{x}_3 \psi_{e0}(\mathbf{x}_3) \Delta V_1(\mathbf{x}_3) \times \int \sum_{n' \neq 0} \frac{\psi_{en'}(\mathbf{x}_3) \psi_{en'}^*(\mathbf{x}_1)}{E_{e0} - E_{en'}} \Delta V_2(\mathbf{x}_1) \psi_{e0}(\mathbf{x}_1) d\mathbf{x}_1, \quad (63)$$

where $\Delta V_1(\mathbf{x}_3)$ is defined by (51) and $\Delta V_2(\mathbf{x}_1)$ (21). Integrating into (63) over all coordinates, we get the following result in leading order in (W_e/W_μ) :

$$b_{\text{vp, sopt}}^{(2)}(n=0) = -v_F \frac{\alpha m_e}{W_e} \frac{W_e^2}{48\pi W_\mu^2} \int_1^\infty \rho(\xi) \xi d\xi \frac{32 + 63\gamma + 44\gamma^2 + 11\gamma^3}{(1+\gamma)^4}. \quad (64)$$

This integral also diverges for large values of ξ . But the sum of the integrals (62) and (64) is finite,

$$b_{\text{vp, sopt}}^{(1)}(n=0) + b_{\text{vp, sopt}}^{(2)}(n=0) = v_F \frac{\alpha W_e}{48\pi W_\mu} \int_1^\infty \rho(\xi) d\xi \frac{11 + 12\gamma + 3\gamma^2}{(1+\gamma)^4}. \quad (65)$$

Let us proceed to the calculation of terms to b with $n \neq 0$. The δ term in the potential (36) gives the following contribution:

$$b_{\text{vp, sopt}}^{(1)}(n \neq 0) = v_F \frac{\alpha}{3\pi} \int_1^\infty \rho(\xi) d\xi \left(-\frac{35W_e}{16W_\mu} \right). \quad (66)$$

The second term in the potential (36) can be simplified by replacing the exact Green's function of the electron with the free one,

$$b_{\text{vp, sopt}}^{(2)}(n \neq 0) = -\frac{16\alpha^3 M_e m_e^2}{9\pi m_e m_\mu} \int_1^\infty \rho(\xi) \xi^2 d\xi \int d\mathbf{x}_2 \int d\mathbf{x}_3 \\ \times \int d\mathbf{x}_4 \psi_{\mu 0}^*(\mathbf{x}_4) \frac{e^{-2m_e \xi |\mathbf{x}_3 - \mathbf{x}_4|}}{|\mathbf{x}_3 - \mathbf{x}_4|} \sum_{n \neq 0} \psi_{\mu n}(\mathbf{x}_4) \psi_{\mu n}(\mathbf{x}_2) |\mathbf{x}_3 - \mathbf{x}_2| \psi_{\mu 0}(\mathbf{x}_2). \quad (67)$$

As a result of analytical integration in (67), we get

$$b_{\text{vp, sopt}}^{(2)}(n \neq 0) = -v_F \frac{\alpha W_e}{3\pi W_\mu} \int_1^\infty \rho(\xi) d\xi \left[\frac{1}{\gamma} - \frac{1}{(1+\gamma)^4} \left(4 + \frac{1}{\gamma} + 10\gamma + \frac{215\gamma^2}{16} + \frac{35\gamma^3}{4} + \frac{35\gamma^4}{16} \right) \right]. \quad (68)$$

The sum of the contributions (66) and (68) is reduced to

$$b_{\text{vp, sopt}}^{(1)}(n \neq 0) + b_{\text{vp, sopt}}^{(2)}(n \neq 0) = -v_F \frac{\alpha W_e}{3\pi W_\mu} \int_1^\infty \rho(\xi) d\xi \frac{35 + 76\gamma + 59\gamma^2 + 16\gamma^3}{16(1+\gamma)^4}. \quad (69)$$

Although the absolute values of the calculated vacuum polarization corrections (42), (48), (49), (52), (56), (65), and (69) are sufficient large, the total contribution is small since the signs of these corrections are different (see Table I).

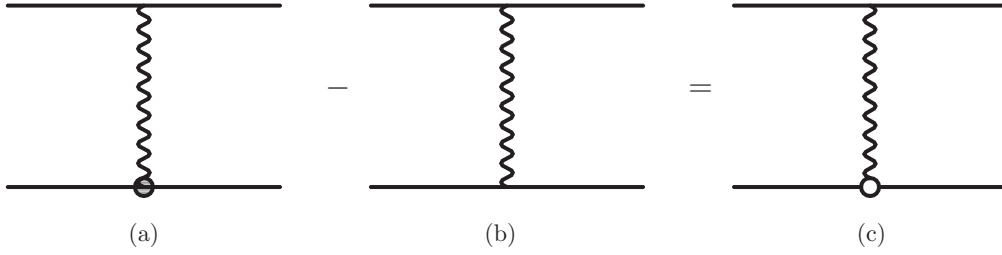


FIG. 4. Nuclear structure correction to the coefficient c in the 1γ interaction. The bold dot in the diagram represents the nucleus vertex operator. The wavy line denotes the hyperfine part of the Breit potential.

The hyperfine interaction (36) contributes to the coefficient c in the second-order perturbation theory. Since the muon coordinate is not included in (36), we immediately set $n = 0$ for muon intermediate states in the Green's function. Then the original formula for this correction is

$$c_{\text{vp, sopt}} = \frac{8\alpha^3 g_N}{9\pi m_e m_p} \int_1^\infty \rho(\xi) d\xi \int d\mathbf{x}_1 \int d\mathbf{x}_3 \int d\mathbf{x}_4 |\psi_{\mu 0}(\mathbf{x}_3)|^2 \psi_{e0}^*(\mathbf{x}_4) \psi_{e0}(\mathbf{x}_1) \times \left[\frac{1}{|\mathbf{x}_3 - \mathbf{x}_4|} - \frac{1}{x_4} \right] G_e(\mathbf{x}_4, \mathbf{x}_1) \left(\pi \delta(\mathbf{x}_1) - \frac{m_e^2 \xi^2}{x_1} e^{-2m_e \xi x_1} \right). \quad (70)$$

After analytical integration over \mathbf{x}_3 as in (21), we split (70) into two parts. The coordinate integration with the δ function is done using (34). In the second term (70), we again use the electronic Green's function in the form (26). The sum of these two terms can be expressed in leading order W_e/W_μ in integral form,

$$c_{\text{vp, sopt}} = \nu_F \frac{\alpha g_N m_\mu W_e}{12\pi m_p W_\mu} \int_1^\infty \rho(\xi) d\xi \frac{3 + 2\frac{m_e \xi}{W_\mu}}{\left(1 + \frac{m_e \xi}{W_\mu}\right)^2}. \quad (71)$$

V. NUCLEAR STRUCTURE AND RECOIL CORRECTION

Another class of corrections in the hyperfine structure of muon-electron ions, which is calculated in this work to increase the calculation accuracy, is determined by the effects of the structure and recoil of the nucleus [48]. We describe the distribution of the charge and magnetic moment of nuclei using the form factors $G_E(k^2)$ and $G_M(k^2)$ in the framework of a simple dipole model,

$$G_E(k^2) = \frac{1}{\left(1 + \frac{k^2}{\Lambda^2}\right)^2}, \quad G_M(k^2) = \frac{G(0)}{\left(1 + \frac{k^2}{\Lambda^2}\right)^2}, \quad G(0) = g_N \frac{m_N}{Z m_p}, \quad (72)$$

where the parameter Λ is related to the nuclear charge radius r_N : $\Lambda = \sqrt{12}/r_N$. In the 1γ interaction, the correction for the nuclear structure to the coefficient c is determined by the interaction amplitude shown in Fig. 4. The point kernel contribution in Fig. 4(b) leads to the hyperfine splitting (13). Then the correction for the nuclear structure is determined by the formula

$$c_{\text{str, } 1\gamma} = -\nu_F \frac{g_e g_N m_\mu}{4m_p} \frac{\left(\frac{2W_e}{\Lambda}\right)^3 + 3\left(\frac{2W_e}{\Lambda}\right)^2 + 3\frac{2W_e}{\Lambda}}{\left(1 + \frac{2W_e}{\Lambda}\right)^3}. \quad (73)$$

The two-photon amplitudes of the electron-nucleus ($e - N$) interaction (see Fig. 5) contribute to a hyperfine splitting of the order of α^5 . It can be represented in integral form in terms of the G_E and G_M form factors, taking into account the subtractive term [48],

$$c_{\text{str, } 2\gamma} = \nu_F \frac{3\alpha M_e m_\mu g_e g_N}{2\pi^2 m_p} \int \frac{d\mathbf{p}}{p^4} \frac{G_M(p)}{G_M(0)} [G_E(p) - 1] = -\nu_F \frac{11Z\alpha M_e m_1 g_e g_N}{16m_p \Lambda}, \quad (74)$$

where the subtractive term contains the magnetic form factor $G_M(p)$. Integration in (74) is performed using the dipole parametrization (72). Other parts of the iterative term $(V_{1\gamma} \times G^f \times V_{1\gamma})_{\text{str}}^{\text{hfs}}$ are used in the second-order perturbation theory (see Fig. 6).

In the second-order perturbation theory, there are two more types of nuclear structure corrections to the coefficient c , shown in Fig. 6. The first contribution is determined by the amplitudes shown schematically in Figs. 6(a) and 6(b), when the hyperfine part of the perturbation operator is determined by the form factor G_M , and the second perturbation operator is expressed in terms of the nucleus charge radius r_N [45],

$$\Delta V_{\text{str, } eN}^C(\mathbf{r}) = \frac{2}{3} \pi Z \alpha r_N^2 \delta(\mathbf{r}). \quad (75)$$

This correction is determined by the following integral expression and can be calculated analytically as follows:

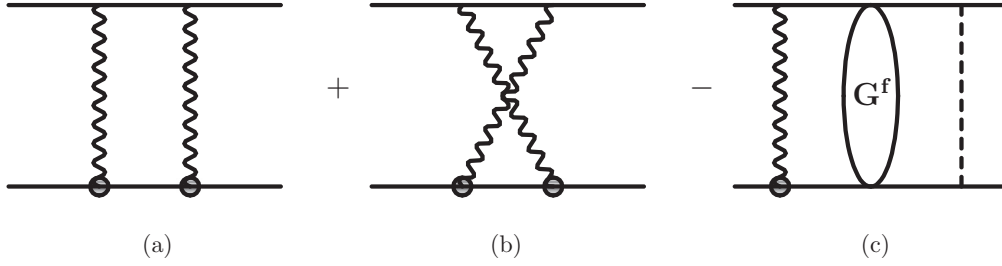


FIG. 5. Nuclear structure correction to the coefficient c from 2γ interactions. The bold dot in the diagram represents the nucleus vertex operator. The wavy line denotes the hyperfine part of the Breit potential. The dotted line corresponds to the Coulomb interaction.

$$\begin{aligned}
 c_{1,\text{str},\text{sopt}}^{eN} &= -v_F \frac{Zr_N^2 W_e^2 g_e g_N m_\mu}{12m_p} \int_0^\infty x^2 dx e^{-x(1+\frac{2W_e}{\Lambda})} \left(-\ln \gamma_1 x + \frac{5}{2} - C - \frac{1}{2} \gamma_1 x \right) \\
 &= -v_F \frac{Zr_N^2 W_e^2 g_e g_N m_\mu}{12m_p} \frac{\left[2 - \frac{2W_e}{\Lambda} + 4\left(1 + \frac{2W_e}{\Lambda}\right) \text{arccth}\left(1 + \frac{4W_e}{\Lambda}\right) \right]}{\left(1 + \frac{2W_e}{\Lambda}\right)^4}.
 \end{aligned} \quad (76)$$

Numerically, this contribution $c_{1,\text{str},\text{sopt}}^{eN}$ is proportional to the square of the charge radius of the nuclei for which the following values are used: $r({}_3^7\text{Li}) = 2.4440 \pm 0.0420$ fm, $r({}_4^9\text{Be}) = 2.5190 \pm 0.0120$ fm, $r({}_5^{11}\text{B}) = 2.4060 \pm 0.0294$ fm [49].

The correction for the nuclear structure of the second type from the interaction amplitudes in Figs. 6(c) and 6(d) is calculated using the potential ΔH (2) and the nucleus magnetic form factor. In the case of the amplitude in Fig. 6(c), one can perform integration over the muon coordinate in the muon state with $n = 0$ and over the electron coordinate. After subtracting the point contribution c_1 , we obtain

$$c_{2,\text{str},\text{sopt}}^{eN} = c_0 \frac{4W_e}{(Z-1)\Lambda} \left\{ -\frac{3}{2} + \frac{2W_\mu}{\Lambda} - \frac{3}{2} \left(\frac{2W_\mu}{\Lambda} \right)^3 + \frac{W_e}{W_\mu} \left[-\frac{9}{2} + \frac{10W_\mu}{\Lambda} - \frac{25}{6} \left(\frac{2W_\mu}{\Lambda} \right)^2 \right] \right\}. \quad (77)$$

There is a nucleus structure contribution to b in the second-order perturbation theory, which is shown in Fig. 7. For the Coulomb muon-nucleus interaction, this correction has the form

$$\begin{aligned}
 b_{\text{str},\text{sopt}}^{\mu N} &= \frac{32\pi^2 \alpha^2}{3m_e m_\mu} r_N^2 \frac{1}{\sqrt{\pi}} (W_\mu)^{3/2} \int d\mathbf{x}_3 \psi_{\mu 0}^*(\mathbf{x}_3) |\psi_{e 0}(\mathbf{x}_3)|^2 G_\mu(\mathbf{x}_3, 0, E_{\mu 0}) \\
 &= -v_F \frac{8}{3} W_\mu^2 r_N^2 \left(\frac{3W_e}{2W_\mu} - \frac{11}{2} \frac{W_e^2}{W_\mu^2} + \dots \right),
 \end{aligned} \quad (78)$$

where the integration result is represented as an expansion in W_e/W_μ .

A structurally similar contribution to b arises from the electron-nucleus interaction. It is defined by the following expression:

$$\begin{aligned}
 b_{\text{str},\text{sopt}}^{eN} &= \frac{32\pi^2 \alpha^2}{3m_e m_\mu} r_N^2 \int d\mathbf{x}_1 \int d\mathbf{x}_3 |\psi_{\mu 0}^*(\mathbf{x}_3)|^2 \psi_{e 0}(\mathbf{x}_3) G_e(\mathbf{x}_3, \mathbf{x}_1, E_{e 0}) \psi_{e 0}(\mathbf{x}_1) \delta(\mathbf{x}_1) \\
 &= -v_F \frac{2W_e W_\mu r_N^2}{(Z-1)} \left[1 - \frac{2W_e}{W_\mu} \ln \frac{W_e}{W_\mu} + \frac{W_e^2}{W_\mu^2} \left(6 \ln \frac{W_e}{W_\mu} - 4 \right) + \dots \right].
 \end{aligned} \quad (79)$$

The total nucleus structure correction to b , which is equal to the sum of (78) and (79), is included in Table I.

Since the masses of particles in this three-particle system differ greatly from each other, various corrections for recoil appear in the calculation of the hyperfine structure, which are determined by the ratio of the masses of the particles. Many of the corrections have already been discussed above in the previous sections. The interaction operator in a three-particle system is constructed by us as the sum of pair interactions that were studied earlier when calculating the fine and hyperfine structures of hydrogenlike atoms [46,50–53]. The two-photon electron-muon exchange interaction shown in Fig. 8 gives a

large recoil correction, which is studied in quantum electrodynamics in [46,54]. The electron-muon interaction operator is defined as follows:

$$\Delta V_{\text{rec},\mu e}^{\text{hfs}}(\mathbf{x}_{\mu e}) = -8 \frac{\alpha^2}{m_\mu^2 - m_e^2} \ln \frac{m_\mu}{m_e} (\mathbf{S}_\mu \mathbf{S}_e) \delta(\mathbf{x}_{\mu e}). \quad (80)$$

After averaging the potential (80) over the wave functions (3), we obtain the contribution to the coefficient b ,

$$b_{\text{rec},2\gamma}^{\mu e} = v_F \frac{3\alpha}{\pi} \frac{m_e m_\mu}{m_\mu^2 - m_e^2} \ln \frac{m_\mu}{m_e} \frac{1}{\left(1 + \frac{W_e}{W_\mu}\right)^3}. \quad (81)$$

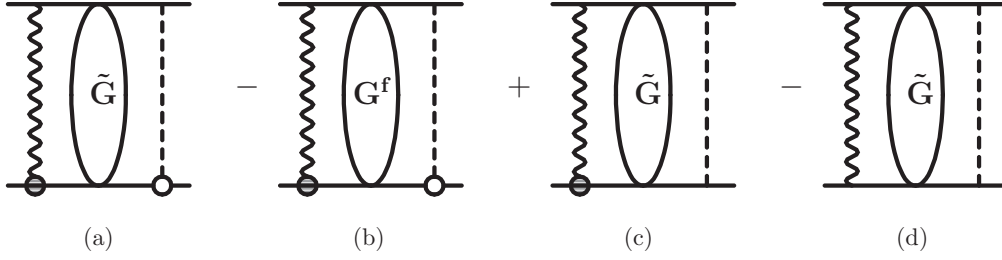


FIG. 6. Nuclear structure correction to the coefficient c in the second order of perturbation theory. The bold dot in the diagram represents the nucleus vertex operator. The wavy line denotes the hyperfine part of the Breit potential. The dotted line corresponds to the Coulomb interaction. \tilde{G} is the reduced Coulomb Green's function.

A similar electron-nucleus 2γ interaction contributes to the coefficient c . In the case of muonic lithium, beryllium, and boron ions, it was studied in [55]. Using the results of [55] [see Eq. (25)], we represent the contribution to c by the following formula:

$$c_{\text{rec},2\gamma}^{eN} = -c_0 \frac{4Z\alpha m_e}{\pi m_2} \ln \frac{m_2}{m_e}. \quad (82)$$

Compared to the main contribution c_0 , this correction contains two small parameters α and m_e/m_μ , but its numerical value slightly increases the accuracy of the result (see Table I).

There are also other three-particle two-photon interactions between particles in muon-electron ions. So, for example, one photon can give a hyperfine interaction between an electron and a muon, and the second can give the Coulomb interaction between an electron and a nucleus (or between a muon and a nucleus). Assuming that such three-particle amplitudes contribute less to the HFS, we include them in the theoretical calculation error.

Let us consider one more correction for nuclear recoil, which is determined by the Hamiltonian ΔH_{rec} (4). The contribution of ΔH_{rec} in the second-order perturbation theory to c is equal to 0, and to the coefficient b it is nonzero and is determined by the electron and muon intermediate P-states,

$$\begin{aligned} \Delta b_{\text{rec},\text{sopt}} = & -\frac{32\pi\alpha^3 M_e M_\mu}{m_e m_\mu M_{\text{Li}}} \int d\mathbf{x}_3 \int d\mathbf{x}_2 \int d\mathbf{x}_1 \Psi_{\mu 0}^*(\mathbf{x}_3) \Psi_{e 0}^*(\mathbf{x}_3) \\ & \times \sum_{n,n' \neq 0} \frac{\Psi_{\mu n}(\mathbf{x}_3) \Psi_{en'}(\mathbf{x}_3) \Psi_{\mu n}^*(\mathbf{x}_2) \Psi_{en'}^*(\mathbf{x}_1)}{E_{\mu 0} + E_{e 0} - E_{\mu n} - E_{en'}} (\mathbf{n}_1 \cdot \mathbf{n}_2) \Psi_{\mu 0}(\mathbf{x}_2) \Psi_{e 0}(\mathbf{x}_1), \end{aligned} \quad (83)$$

where $\mathbf{n}_1, \mathbf{n}_2$ are unit vectors in coordinate space.

For the analytical calculation (82), we replace the electron Green's function with the free one, as in Sec. II,

$$\begin{aligned} \Delta b_{\text{rec},\text{sopt}} = & \frac{16\alpha^3 M_e^2 M_\mu}{m_e m_\mu M_{\text{Li}}} \int d\mathbf{x}_3 \int d\mathbf{x}_2 \int d\mathbf{x}_1 \Psi_{\mu 0}^*(\mathbf{x}_3) \Psi_{e 0}^*(\mathbf{x}_3) \\ & \times \sum_{n \neq 0} \Psi_{\mu n}(\mathbf{x}_3) \Psi_{\mu n}^*(\mathbf{x}_2) \frac{e^{-b|\mathbf{x}_3 - \mathbf{x}_1|}}{|\mathbf{x}_3 - \mathbf{x}_1|} (\mathbf{n}_1 \cdot \mathbf{n}_2) \Psi_{\mu 0}(\mathbf{x}_2) \Psi_{e 0}(\mathbf{x}_1). \end{aligned} \quad (84)$$

After that, we integrate over \mathbf{x}_1 and expand the result over b (or, which is the same, over $\sqrt{M_e/M_\mu}$),

$$\int d\mathbf{x}_1 (\mathbf{n}_1 \cdot \mathbf{n}_2) \frac{e^{-b|\mathbf{x}_3 - \mathbf{x}_1|}}{|\mathbf{x}_3 - \mathbf{x}_1|} = 2\pi (\mathbf{n}_2 \cdot \mathbf{n}_3) \left[\frac{4x_3}{3b} - \frac{x_3^2}{2} + \frac{2bx_3^3}{15} + \dots \right]. \quad (85)$$

After that, we take the first term in square brackets (84), perform the integration over the angular variables, and introduce dimensionless variables in the integrals with radial functions,

$$\delta b_{\text{rec},\text{sopt}} = \nu_F \frac{64M_e}{9M_{\text{Li}}} \sqrt{\frac{M_e}{M_\mu}} \sum_{n>1} \frac{n}{\sqrt{n^2 - 1}} \int_0^\infty x_3^3 R_{10}(x_3) R_{n1}(x_3) dx_3 \int_0^\infty x_2^2 R_{10}(x_2) R_{n1}(x_2) dx_2. \quad (86)$$

Two contributions from discrete and continuous spectra in (85) have the form

$$\delta b_{\text{rec},\text{sopt}}^{(1)d} = \nu_F \frac{2^{11}M_e}{9M_{\text{Li}}} \sqrt{\frac{M_e}{M_\mu}} \sum_{n>1} \frac{n^6(n-1)^{2n-\frac{9}{2}}}{(n+1)^{2n+\frac{9}{2}}}, \quad (87)$$

$$\delta b_{\text{rec},\text{sopt}}^{(1)c} = \nu_F \frac{2^{11}M_e}{9M_{\text{Li}}} \sqrt{\frac{M_e}{M_\mu}} \int_0^\infty \frac{ke^{-\frac{4}{k}\text{arctg}(k)} dk}{(1 - e^{-2\pi/k})(k^2 + 1)^{3/2}}. \quad (88)$$

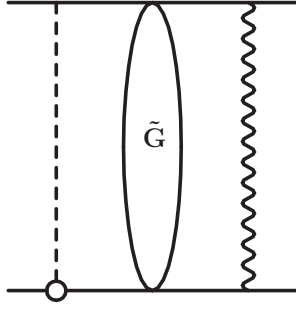


FIG. 7. Correction to the nucleus structure to b in the second-order perturbation theory. The wavy line denotes the hyperfine ($e - \mu$) interaction. \tilde{G} is the reduced Coulomb Green's function.

The calculation of the second expansion term in (84) gives the following result:

$$\delta b_{\text{rec,sopt}}^{(2)} = -\nu_F \frac{W_e M_e}{W_\mu M_{\text{Li}}}, \quad (89)$$

which is two orders of magnitude smaller than (86) and (87).

VI. ELECTRON VERTEX CORRECTION

The main contribution of the order of α^4 to the hyperfine structure (the coefficient b) is determined by the interaction operator (7), as discussed in Sec. II. Among different corrections to (7), there is a correction determined by the electron vertex function, which is shown in Fig. 9(a). To calculate this

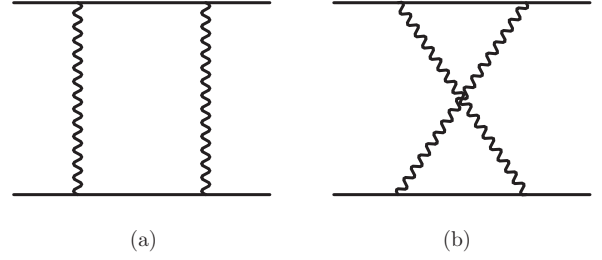


FIG. 8. Two-photon exchange amplitudes of the electron-muon hyperfine interaction.

contribution, it is first convenient to write it in the momentum representation,

$$\Delta V_{\text{vert}}^{\text{hfs}}(k^2) = -\frac{8\alpha^2}{3m_e m_\mu} [G_M^{(e)}(k^2) - 1] (\mathbf{S}_e \mathbf{S}_\mu), \quad (90)$$

where $G_M^{(e)}(k^2)$ is the magnetic form factor of the electron, and the factor α/π is separated from the factor $[G_M^{(e)}(k^2) - 1]$ for convenience. The commonly used approximation, when the magnetic form factor is approximately replaced by its value at zero, $G_M^{(e)}(k^2) \approx G_M^{(e)}(0) = 1 + \kappa_e$, is not applicable in this case. Since the typical momentum of an exchange photon is $k \sim \alpha M_\mu$, we cannot neglect it in $G_M^{(e)}(k^2)$ as compared to the electron mass m_e . Therefore, it is necessary to use the exact expression for the Pauli form factor $g(k^2)$ [$G_M^{(e)}(k^2) - 1 \approx g(k^2)$] [47].

Using the Fourier transform of the potential (90) and averaging it over the wave functions (6), one can represent the electron vertex correction in the HFS as an integral,

$$b_{\text{vert}, 1\gamma} = \nu_F \frac{\alpha(1 + \kappa_\mu)m_e^3 W_e}{2\pi^2 W_\mu^4} \int_0^\infty g(k^2) k^2 dk \times \left\{ \left[1 + \left(\frac{m_e}{2W_\mu} \right)^2 k^2 \right]^2 \left[\left(\frac{W_e}{W_\mu} \right)^2 + \left(\frac{m_e}{2W_\mu} \right)^2 k^2 \right]^2 \right\}^{-1}. \quad (91)$$

The contribution (91) is of the order of $O(\alpha^5 M_e/M_\mu)$. The numerical value (91) is obtained after integration over k with a one-loop expression for the form factor $g(k^2)$ [47] (see the results in Table I). Using $g(k^2 = 0)$, we obtain the values of the electron vertex corrections: 41.6139 MHz (μeLi), 140.2879 MHz (μeBe), 332.3111 MHz (μeB), which differ from (91) by approximately 2.5%.

The contribution of the potential (90) to b in the second-order perturbation theory is shown in Fig. 9(b). In this case, the second perturbation potential is determined by ΔH (3) (dotted line in the diagram). Let us divide the total contribution of the amplitude in Fig. 9(b) into two parts, which correspond to the muon in the ground state ($n = 0$) and the muon in the excited

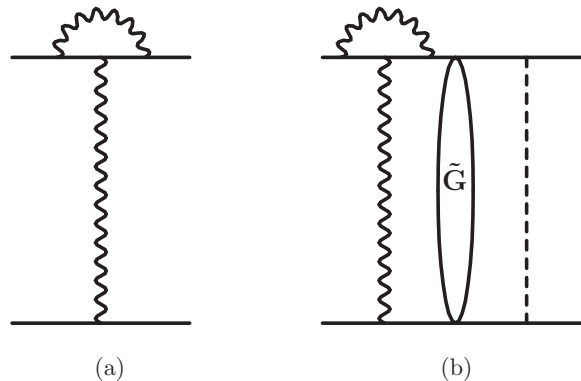


FIG. 9. Electron vertex correction in the first and second orders of perturbation theory. The Coulomb photon is represented by a dotted line. The wavy line represents the hyperfine part of the Breit potential. \tilde{G} is the reduced Coulomb Green's function.

intermediate state ($n \neq 0$). The first contribution with $n = 0$ becomes equal to

$$b_{\text{vert, sopt}}(n=0) = \frac{8\alpha^2}{3\pi^2 m_e m_\mu} \int_0^\infty k [G_M^{(e)}(k^2) - 1] dk \int d\mathbf{x}_1 \int d\mathbf{x}_3 \psi_{e0}(\mathbf{x}_3) \times \Delta \tilde{V}_1(k, \mathbf{x}_3) G_e(\mathbf{x}_1, \mathbf{x}_3) V_\mu(\mathbf{x}_1) \psi_{e0}(\mathbf{x}_1), \quad (92)$$

where $V_\mu(\mathbf{x}_1)$ is determined by (21), and

$$\Delta \tilde{V}_1(k, \mathbf{x}_3) = \int d\mathbf{x}_4 \psi_{\mu 0}^*(\mathbf{x}_4) \frac{\sin(k|\mathbf{x}_3 - \mathbf{x}_4|)}{|\mathbf{x}_3 - \mathbf{x}_4|} \psi_{\mu 0}(\mathbf{x}_4) = \frac{\sin(kx_3)}{x_3} \frac{1}{\left[1 + \frac{k^2}{(2W_\mu)^2}\right]^2}. \quad (93)$$

After substituting the electron Green's function (30) into (92), we reduce this expression to an integral form,

$$\begin{aligned} b_{\text{vert, sopt}}(n=0) = v_F \frac{\alpha}{2\pi^2} \left(\frac{m_e}{W_\mu}\right)^2 \left(\frac{W_e}{W_\mu}\right)^2 \int_0^\infty \frac{k [G_M^{(e)}(k^2) - 1] dk}{\left[1 + \frac{m_e^2 k^2}{(2W_\mu)^2}\right]^2} \\ \times \int_0^\infty x_3 e^{-\frac{W_e}{W_\mu} x_3} \sin\left(\frac{m_e k}{2W_\mu} x_3\right) dx_3 \int_0^\infty x_1 \left(1 + \frac{x_1}{2}\right) e^{-x_1 \left(1 + \frac{W_e}{W_\mu}\right)} dx_1 \left[\frac{W_\mu}{W_e x_3} - \ln\left(\frac{W_e}{W_\mu} x_3\right) \right. \\ \left. - \ln\left(\frac{W_e}{W_\mu} x_3\right) + \text{Ei}\left(\frac{W_e}{W_\mu} x_3\right) + \frac{7}{2} - 2C - \frac{W_e}{W_\mu} \frac{(x_1 + x_3)}{2} + \frac{1 - e^{\frac{W_e}{W_\mu} x_3}}{\frac{W_e}{W_\mu} x_3} \right]. \end{aligned} \quad (94)$$

All integrations over the coordinates x_1, x_3 are performed analytically, and over k numerically. The intermediate expression before integration over k is omitted since it has a cumbersome form.

The second part of the vertex correction [Fig. 9(b)] with $n \neq 0$ after a series of simplifications can be transformed into

$$\begin{aligned} b_{\text{vert, sopt}}(n \neq 0) = v_F \frac{W_e W_\mu^3}{\pi^3 (Z-1)} \int e^{-W_\mu x_2} d\mathbf{x}_2 \int e^{-W_e x_3} d\mathbf{x}_3 \int e^{-W_\mu x_4} d\mathbf{x}_4 \\ \times \int_0^\infty k \sin(k|\mathbf{x}_3 - \mathbf{x}_4|) [G_M^{(e)}(k^2) - 1] \frac{|\mathbf{x}_3 - \mathbf{x}_2|}{|\mathbf{x}_3 - \mathbf{x}_4|} [\delta(\mathbf{x}_4 - \mathbf{x}_2) - \psi_{\mu 0}(\mathbf{x}_4) \psi_{\mu 0}(\mathbf{x}_2)]. \end{aligned} \quad (95)$$

The contributions of the two terms in square brackets (95) will be presented separately after integration over the coordinates \mathbf{x}_1 and \mathbf{x}_3 ($\gamma_2 = m_e k / 2W_\mu$):

$$\begin{aligned} b_{\text{vert, sopt}}^{(1)}(n \neq 0) = v_F \frac{\alpha}{2\pi^2} \left(\frac{m_e}{W_\mu}\right)^3 \frac{W_e}{(Z-1)W_\mu} \int_0^\infty k^2 [G_M^{(e)}(k^2) - 1] dk \frac{1}{(\gamma_1^2 - 1)^3} \\ \times \left[\frac{4\gamma_1(\gamma_1^2 - 1)}{(1 + \gamma_2^2)^3} - \frac{\gamma_1(3 + \gamma_1^2)}{(1 + \gamma_2^2)^2} + \frac{4\gamma_1^2(\gamma_1^2 - 1)}{(\gamma_1^2 + \gamma_2^2)^3} + \frac{1 + 3\gamma_1^2}{(\gamma_1^2 + \gamma_2^2)^2} \right], \end{aligned} \quad (96)$$

$$\begin{aligned} b_{\text{vert, sopt}}^{(2)}(n \neq 0) = -v_F \frac{\alpha}{2\pi^2} \left(\frac{m_e}{W_\mu}\right)^3 \frac{W_e}{(Z-1)W_\mu} \int_0^\infty k^2 [G_M^{(e)}(k^2) - 1] dk \\ \times \frac{1}{(1 + \gamma_2^2)^2} \left\{ \frac{2}{(\gamma_1^2 + \gamma_2^2)} - \frac{(\gamma_1 + 1)}{[(1 + \gamma_1)^2 + \gamma_2^2]^2} - \frac{2}{(\gamma_1 + 1)^2 + \gamma_2^2} - \frac{\gamma_2^2 - 3\gamma_1^2}{(\gamma_1^2 + \gamma_2^2)^3} \right\}. \end{aligned} \quad (97)$$

Note that the theoretical error in the sum of contributions $b_{\text{vert, sopt}}^{(1)}(n \neq 0) + b_{\text{vert, sopt}}^{(2)}(n \neq 0)$ is determined by the factor $\sqrt{M_e/M_\mu}$ connected with the omitted terms in the expansion of the form (27). It can be about 10% of the total (96) and (97) result, which is represented by a separate line in Table I.

The considered electron vertex corrections in hyperfine splitting are of the order of α^5 . The total value of the resulting vertex contribution (see Table I) differs from the above values in the approximation when the form factor $g(k^2)$ is replaced by the anomalous magnetic moment of the electron.

VII. CONCLUSION

In this paper, we calculate the intervals of the hyperfine structure of the ground state for muon-electron ions of lithium, beryllium, boron, and helium using the perturbation theory method formulated earlier for muonic helium ions in Refs. [31,32]. To increase the accuracy of the calculations, we took into account corrections in the hyperfine structure of orders α^5 and α^6 , connected with the effects of vacuum polarization, the nucleus structure and recoil, and electron vertex corrections. All obtained numerical results are presented in Table I. It specifies the correction values for lithium,

beryllium, and boron ions with an accuracy of two decimal places, and for muonic helium with an accuracy of four decimal places. This is due to the increase in the total value of contributions due to the nuclear charge Z during the transition from muon-electron helium to boron.

Let us note the main features of the performed calculations:

(1) Muon-electron ions of lithium, beryllium, and boron have a complex hyperfine structure in the ground state, which arises as a result of the interaction of the magnetic moments of the nucleus, electron, and muon. We have explored small intervals of the hyperfine structure that can be measured.

(2) When calculating the HFS, there are small parameters of the fine-structure constant and the particle mass ratio which can be used in constructing expansions in perturbation theory. In this paper, corrections of the order of α^4 , α^5 , and α^6 are considered, taking into account the recoil effects of the first and second orders.

(3) Vacuum polarization effects are of great importance for achieving high accuracy in the calculation of hyperfine splitting. They lead to a modification of the two-particle interaction potentials, which give corrections of the order of $\alpha^5 \frac{M_e}{M_\mu}$. We take into account the contribution of one-loop vacuum polarization in the first and second orders of perturbation theory.

(4) The electron vertex correction to the coefficient b is obtained taking into account the one-loop expression for the magnetic form factor of the electron since the characteristic momentum entering the vertex operator is of the order of the electron mass.

(5) Corrections for the structure of the nucleus are expressed both in terms of electromagnetic form factors and in terms of the charge radius.

(6) Relativistic corrections to the coefficients b and c are obtained using expressions from [20],

$$b_{\text{rel}} = \left[1 + \frac{3}{2}(Z-1)^2\alpha^2 - \frac{1}{3}(Z\alpha)^2 \right] v_F, \\ c_{\text{rel}} = \frac{3}{2}(Z-1)^2\alpha^2 c_0. \quad (98)$$

(7) To estimate the radiative corrections without recoil of the order of $O(\alpha^6)$ in the HFS, we use the results of analytical calculations in two-particle atoms [50–53], which give the following expressions for b and c :

$$b_{\alpha^2} = \alpha^2 v_F \left(\ln 2 - \frac{5}{2} \right), \quad c_{\alpha^2} = \frac{1}{2} \alpha (Z\alpha) \left(\ln 2 - \frac{5}{2} \right) c_0. \quad (99)$$

An analysis of individual contributions to the hyperfine-structure coefficients b and c in Table I shows that relativistic corrections, corrections for nucleus structure and recoil, vacuum polarization, and electron vertex corrections must be taken into account to achieve good calculation accuracy. The theoretical uncertainty can be estimated in terms of the Fermi energy v_F and the parameters W_e and W_μ . The main source of the theoretical error is determined by recoil corrections of orders $(W_e/W_\mu)^2 v_F$, $(W_e/W_\mu)^{5/2} \ln(W_e/W_\mu) v_F$, which are not always taken into account exactly in the calculations. So, for muonic helium-3,4, the error is about 0.029 MHz; for lithium, it is 0.41 MHz; for beryllium, it is 1.74 MHz; and for boron, it is 4.68 MHz. To obtain this estimate, we add the two above-mentioned uncertainties in quadrature.

Using the total numerical values for the coefficients b and c presented in Table I, we obtain the following values for the hyperfine intervals for lithium, beryllium, and boron (20): $\Delta v_1(\mu e_3^7 \text{Li}) = 13\,994.76(41)$ MHz, $\Delta v_1(\mu e_4^9 \text{Be}) = 85\,539.16(1.74)$ MHz, $\Delta v_1(\mu e_5^{11} \text{B}) = 123\,767.56(4.68)$ MHz, and $\Delta v_2(\mu e_3^7 \text{Li}) = 21\,731.04(41)$ MHz, $\Delta v_2(\mu e_4^9 \text{Be}) = 35\,067.07(1.74)$ MHz, $\Delta v_2(\mu e_5^{11} \text{B}) = 162\,228.31(4.68)$ MHz.

In the case of muonic helium, the hyperfine splitting of the ground state has the form $\Delta v(\mu e_2^3 \text{He}) = \frac{3}{4}(b-c) = 4166.089(29)$ MHz, $\Delta v(\mu e_2^4 \text{He}) = 4464.504(29)$ MHz.

These numerical values agree with the experimental data (2), taking into account the available theoretical and experimental errors. Our results are also in good agreement with recent calculations using the variational method in Ref. [56]: 4166.39(58) MHz ($\mu e_2^3 \text{He}$), 4464.55(60) MHz ($\mu e_2^4 \text{He}$).

Previously, the calculation of hyperfine intervals in the muonic lithium-7 ion was performed in Refs. [23,24] within the framework of the variational method. Our results generally agree with the results [24] on muon-electron lithium-7: $\Delta v_1(\mu e_3^7 \text{Li}) = 13\,989.19$ MHz, $\Delta v_2(\mu e_3^7 \text{Li}) = 21\,729.22$ MHz. A slight difference is due to the inclusion in our work of corrections for the vacuum polarization and the structure of the nucleus. In the case of muon-electron helium, the results [24] of the hyperfine splitting of the ground state, $\Delta v(\mu e_2^3 \text{He}) = 4166.383$ MHz, $\Delta v(\mu e_2^4 \text{He}) = 4464.554$ MHz, differ from our values by approximately 0.29 MHz ($\mu e_2^3 \text{He}$) and 0.05 MHz ($\mu e_2^4 \text{He}$).

We performed an analytical calculation of recoil corrections of orders $\frac{W_e^2}{W_\mu^2} \ln \frac{W_e}{W_\mu}$, $\frac{W_e^2}{W_\mu^2}$ from several sources. As already noted, in Ref. [31] the recoil corrections (24) were calculated numerically for muonic helium-4. The sum of (23) and (24) contributions obtained in Ref. [31] is (-29.65) MHz. In our work, a similar contribution is determined by the sum of (-29.8306) MHz and 0.0935 MHz [(A7)] (see Table I) and is equal to (-29.7371) MHz, which differs from the result [31] by 0.087 MHz.

ACKNOWLEDGMENTS

The work was supported by the Foundation for the Advancement of Theoretical Physics and Mathematics “BASIS,” Grant No. 19-1-5-67-1 (F.A.M.).

APPENDIX: THE ESTIMATION OF OTHER RECOIL CONTRIBUTIONS TO THE COEFFICIENT (24)

As noted in Sec. II, the contribution to (24) is calculated using the approximation of the free Green’s function for the electron G_e^0 . The following term $G_e^0 V^C G_e^0$ in the expansion of the Green’s function contributes to the coefficient $b_1(n \neq 0)$ in (24) of the form

$$b_1^{(2)}(n \neq 0) = -\frac{\alpha W_e^2 g_e g_\mu}{3\pi(Z-1)m_e m_1} |\psi_{e0}(0)|^2 \int \psi_{\mu 0}(\mathbf{x}_3) d\mathbf{x}_3 \\ \times \int \psi_{\mu 0}(\mathbf{x}_2) d\mathbf{x}_2 \sum_{n \neq 0} \psi_{\mu n}(\mathbf{x}_3) \psi_{\mu n}(\mathbf{x}_2) \\ \times \int \frac{d\mathbf{x}}{|\mathbf{x}|} \int \frac{d\mathbf{x}_1}{|\mathbf{x}_2 - \mathbf{x}_1|} \frac{e^{-\beta|\mathbf{x} - \mathbf{x}_3|}}{|\mathbf{x} - \mathbf{x}_3|} \frac{e^{-\beta|\mathbf{x} - \mathbf{x}_1|}}{|\mathbf{x} - \mathbf{x}_1|}. \quad (\text{A1})$$

After calculating the integral over \mathbf{x}_1 , we use the expansion over $\beta|\mathbf{x} - \mathbf{x}_2|$, as in (27). The first term $1/\beta$ of the expansion does not contribute due to the orthogonality of the muon

wave functions, while the second term gives the following correction:

$$b_1^{(2)}(n \neq 0) = \frac{2\alpha W_e^2 g_e g_\mu}{3(Z-1)m_e m_1} |\psi_{e0}(0)|^2 \int \psi_{\mu 0}(\mathbf{x}_3) d\mathbf{x}_3 \int \psi_{\mu 0}(\mathbf{x}_2) d\mathbf{x}_2 \times \sum_{n \neq 0} \psi_{\mu n}(\mathbf{x}_3) \psi_{\mu n}(\mathbf{x}_2) I(\mathbf{x}_2, \mathbf{x}_3), \quad I(\mathbf{x}_2, \mathbf{x}_3) = \int d\mathbf{x} \frac{|\mathbf{x} - \mathbf{x}_2|}{|\mathbf{x}|} \frac{e^{-\beta|\mathbf{x} - \mathbf{x}_3|}}{|\mathbf{x} - \mathbf{x}_3|}. \quad (\text{A2})$$

Let us expand the integral $I(\mathbf{x}_2, \mathbf{x}_3)$ into a series for small values of x_2^i ,

$$I(\mathbf{x}_2, \mathbf{x}_3) = I(0) + x_2^i I_i(0) + \frac{1}{2} x_2^i x_2^j I_{ij}(0), \quad I_i(0) = \frac{dI}{dx_2^i} \Big|_{x_2^i=0} = 0, \quad I_{ij}(0) = \frac{d^2 I}{dx_2^i dx_2^j} \Big|_{x_2^i=0} = 0. \quad (\text{A3})$$

Using the exact form of $I(\mathbf{x}_2, \mathbf{x}_3)$, let us calculate $I_i(0)$, $I_{ij}(0)$ and obtain

$$I(\mathbf{x}_2, \mathbf{x}_3) = \frac{8\pi}{\beta^2} - (\mathbf{x}_2 \mathbf{x}_3) \frac{4\pi}{9} \left[-4 + 3C + \frac{3}{2} \ln \frac{M_e}{M_\mu} + 3 \ln(W_\mu x_3) + \frac{3}{2} \ln \frac{n^2 - 1}{n^2} \right] + \frac{\pi}{6} \left\{ [x_2^2 \ln(W_\mu x_3) - \frac{(\mathbf{x}_2 \mathbf{x}_3)^2}{x_3^2} \left[11 - 9C - 9 \ln(W_\mu x_3) - \frac{9}{2} \ln \frac{M_e}{M_\mu} \right]] \right\}. \quad (\text{A4})$$

Separating the terms dependent and independent of n and calculating the corresponding matrix elements in the same way as in Sec. II, we obtain the following additional correction to the coefficient $b_1(n \neq 0)$:

$$b_1^{(2)}(n \neq 0) = -v_F \frac{W_e^2}{3(Z-1)W_\mu^2 g_\mu} \frac{g_e}{g_\mu} 4 \left[\frac{7}{4} + \frac{3}{2} \ln \frac{M_e}{4M_\mu} + S_{ln}^d + S_{ln}^c \right], \quad (\text{A5})$$

$$S_{ln}^d = 2^{11} \sum_{n>1} \ln \frac{n^2 - 1}{n^2} \frac{n^7(n-1)^{2n-5}}{(n+1)^{2n+5}}, \quad S_{ln}^c = 2^{11} \int_0^\infty \ln(k^2 + 1) \frac{k dk}{(k^2 + 1)^5 (1 - e^{-\frac{2\pi}{k}})} e^{-\frac{4}{k} \arctan k}. \quad (\text{A6})$$

The numerical values of the correction (A5) for the considered ions are

$$b_1^{(2)}(n \neq 0) = \begin{cases} 0.65 \text{ MHz}, & \mu e_3^7 \text{ Li} \\ 1.84 \text{ MHz}, & \mu e_4^9 \text{ Be} \\ 3.71 \text{ MHz}, & \mu e_5^{11} \text{ B} \\ 0.0951 \text{ MHz}, & \mu e_2^3 \text{ He} \\ 0.0935 \text{ MHz}, & \mu e_2^4 \text{ He}. \end{cases} \quad (\text{A7})$$

They are taken into account when obtaining the total result in Table I.

-
- [1] A. Antognini, F. Kottmann, F. Biraben *et al.*, *Ann. Phys.* **331**, 127 (2013).
 - [2] J. Krauth, M. Diepold, B. Franke *et al.*, *Ann. Phys.* **366**, 168 (2016).
 - [3] M. Diepold, B. Franke, J. Krauth *et al.*, *Ann. Phys.* **396**, 220 (2018).
 - [4] J. J. Krauth, K. Schuhmann, M. A. Ahmed *et al.*, *Nature (London)* **589**, 527 (2021).
 - [5] A. Antognini, F. Kottmann, and R. Pohl, *SciPost Phys. Proc.* **5**, 021 (2021).
 - [6] E. Tiesinga, P. J. Mohr, D. B. Newell, and B. N. Taylor, *Rev. Mod. Phys.* **93**, 025010 (2021).
 - [7] S. Schmidt, M. Willig, J. Haack *et al.*, *J. Phys.: Conf. Ser.* **1138**, 012010 (2018).
 - [8] A. Beyer, L. Maisenbacher, A. Matveev *et al.*, *Science* **358**, 79 (2017).
 - [9] W. Xiong, A. Gasparian, H. Gao *et al.*, *Nature (London)* **575**, 147 (2019).
 - [10] N. Bezginov, T. Valdez, M. Horbatsch *et al.*, *Science* **365**, 1007 (2019).
 - [11] H. Fleurbaey, S. Galtier, S. Thomas, M. Bonnaud, L. Julien, F. Biraben, F. Nez, M. Abgrall, and J. Guena, *Phys. Rev. Lett.* **120**, 183001 (2018).
 - [12] R. Gilman, E. J. Downie, G. Ron *et al.* (MUSE Collaboration), *arXiv:1709.09753*.
 - [13] P. Strasser, M. Abe, M. Aoki *et al.*, *EPJ Web Conf.* **198**, 00003 (2019).
 - [14] P. Crivelli, *Hyperfine Interact.* **239**, 49 (2018).
 - [15] P. Strasser, K. Shimomura, and H. A. Torii, *JPS Conf. Proc.* **21**, 011045 (2018).
 - [16] C. Pizzolotto, A. Adamczak, D. Bakalov *et al.*, *Eur. Phys. J. A* **56**, 185 (2020).

- [17] P. Amaro, A. Adamczak, M. Abdou Ahmed *et al.*, [arXiv:2112.00138](#).
- [18] B. Abi, T. Albahri, S. Al-Kilani *et al.*, *Phys. Rev. Lett.* **126**, 141801 (2021).
- [19] M. Abe *et al.*, *Prog. Theor. Expt. Phys.* **2019**, 053C02 (2019).
- [20] K.-N. Huang and V. W. Hughes, *Phys. Rev. A* **26**, 2330 (1982).
- [21] R. J. Drachman, *Phys. Rev. A* **22**, 1755 (1980).
- [22] M.-K. Chen, *J. Phys. B* **26**, 2263 (1993).
- [23] A. M. Frolov, *Phys. Rev. A* **61**, 022509 (2000).
- [24] A. M. Frolov, *Phys. Lett. A* **357**, 334 (2006).
- [25] V. I. Korobov, *Phys. Rev. A* **61**, 064503 (2000).
- [26] A. V. Eskin, V. I. Korobov, A. P. Martynenko, and V. V. Sorokin, *J. Phys.: Conf. Ser.* **1690**, 012092 (2020).
- [27] V. I. Korobov, *Phys. Part. Nucl.* **53**, 5 (2022).
- [28] G. W. F. Drake and Z.-C. Yan, *Phys. Rev. A* **46**, 2378 (1992).
- [29] M. Gladish *et al.*, in *Proceedings of the 8th International Conference on Atomic Physics*, edited by I. Lindgren, A. Rosen, and S. Svanberg (Plenum, New York, 1983).
- [30] C. J. Gardner, A. Badertscher, W. Beer, P. R. Bolton, P. O. Egan, M. Gladisch, M. Greene, V. W. Hughes, D. C. Lu, F. G. Mariam, P. A. Souder, H. Orth, J. Vetter, and G. zu Putlitz, *Phys. Rev. Lett.* **48**, 1168 (1982).
- [31] S. D. Lakdawala and P. J. Mohr, *Phys. Rev. A* **29**, 1047 (1984).
- [32] S. D. Lakdawala and P. J. Mohr, *Phys. Rev. A* **24**, 2224 (1981).
- [33] E. Borie, *Z. Phys. A* **291**, 107 (1979).
- [34] V. L. Yakhontov and M. Ya. Amusia, *J. Phys. B* **16**, L71 (1983).
- [35] A. A. Krutov and A. P. Martynenko, *Phys. Rev. A* **78**, 032513 (2008).
- [36] A. A. Krutov and A. P. Martynenko, *Phys. Rev. A* **86**, 052501 (2012).
- [37] S. G. Karshenboim, V. G. Ivanov, and V. I. Korobov, *Phys. Rev. A* **97**, 022504 (2018).
- [38] A. E. Dorokhov, V. I. Korobov, A. P. Martynenko, and F. A. Martynenko, *Phys. Rev. A* **103**, 052806 (2021).
- [39] I. I. Sobel'man, *Introduction to the Theory of Atomic Spectra* (Pergamon Press, NY, 1972).
- [40] N. J. Stone, *At. Data Nucl. Data Tables* **90**, 75 (2005).
- [41] H. F. Hameka, *J. Chem. Phys.* **47**, 2728 (1967).
- [42] H. A. Bethe and E. E. Salpeter, *Quantum Mechanics of One- and Two-electron Atoms* (Springer, Berlin, 1957).
- [43] A. A. Krutov, A. P. Martynenko, F. A. Martynenko, and O. S. Sukhorukova, *Phys. Rev. A* **94**, 062505 (2016).
- [44] A. P. Martynenko, F. A. Martynenko, and R. N. Faustov, *J. Expt. Theor. Phys.* **124**, 895 (2017) [*Zh. Eksp. Teor. Fiz.* **151**, 1052 (2017)].
- [45] A. A. Krutov, A. P. Martynenko, G. A. Martynenko, and R. N. Faustov, *J. Expt. Theor. Phys.* **120**, 73 (2015) [*Zh. Eksp. Teor. Fiz.* **147**, 85 (2015)].
- [46] M. I. Eides, H. Grotch, and V. A. Shelyuto, *Phys. Rep.* **342**, 62 (2001); *Theory of Light Hydrogenic Bound States*, Springer Tracts in Modern Physics, Vol. 222 (Springer, Berlin, 2007).
- [47] V. B. Berestetskii, E. M. Lifshits and L. P. Pitaevskii, *Quantum Electrodynamics* (Nauka, Moscow, 1980).
- [48] R. N. Faustov and A. P. Martynenko, *Phys. Rev. A* **67**, 052506 (2003); *Phys. At. Nucl.* **67**, 457 (2004); [*Yad. Fiz.* **67**, 477 (2004)].
- [49] I. Angeli and K. P. Marinova, *At. Data Nucl. Data Tables* **99**, 69 (2013).
- [50] S. J. Brodsky and G. W. Erickson, *Phys. Rev.* **148**, 26 (1966).
- [51] N. Kroll and F. Pollack, *Phys. Rev.* **84**, 594 (1951).
- [52] R. Karplus, A. Klein, and J. Schwinger, *Phys. Rev.* **84**, 597 (1951).
- [53] W. A. Newcomb and E. E. Salpeter, *Phys. Rev.* **97**, 1146 (1955).
- [54] R. Arnowitt, *Phys. Rev.* **92**, 1002 (1953).
- [55] A. E. Dorokhov, A. A. Krutov, A. P. Martynenko, F. A. Martynenko, and O. S. Sukhorukova, *Phys. Rev. A* **98**, 042501 (2018).
- [56] D. T. Aznabayev, A. K. Bekbaev, and V. I. Korobov, *Phys. Part. Nucl. Lett.* **15**, 236 (2018).